Title: Modelling irruptive species with hybrid machine learning: A case study of crown-of-thorns starfish outbreaks on the Great Barrier Reef

Short title: Forecasting crown-of-thorns starfish irruptions with hybrid modelling

Owen Stewart*[1], Samuel A. Matthews[2,3], David J. Warne[1,4], and Michael Bode[1,5]

[1]School of Mathematical Sciences, Queensland University of Technology, Brisbane, Queensland, 4000, Australia
[2]Australian Institute of Marine Science, Cape Cleveland, Queensland, 4810, Australia
[3]Great Barrier Reef Marine Park Authority, Townsville, Queensland, 4810, Australia
[4]Centre for Data Science, Queensland University of Technology, Brisbane, Queensland, 4000, Australia
[5]Securing Antarctica's Environmental Future, Queensland University of Technology, Brisbane, Queensland, 4000, Australia
*Corresponding Author: owen.stewart@hdr.qut.edu.au

ORCiD:
Owen Stewart: https://orcid.org/0009-0005-1589-9551
Samuel A. Matthews: https://orcid.org/0000-0003-1936-1220
David J. Warne: https://orcid.org/0000-0002-9225-175X
Michael Bode: https://orcid.org/0000-0002-5886-4421

Abstract:

Irruptions consist of rapid and severe increases in abundance, which for some species can result in significant economic and environmental damage. Forecasting the timing and location of these irruptions is crucial for effective management, however is difficult due to the complexity of the ecosystems in which they occur and the conditions under which they arise. Hybrid machine learning (ML) modelling has the potential to offer more accurate predictions than standard mechanistic, statistical, and ML approaches by combining the flexibility of ML with existing mechanistic knowledge. In this paper we develop a hybrid forecasting model for crown-of-thorns starfish (COTS) irruptions which contribute substantially to ecosystem degradation on the Great Barrier Reef (GBR). The hybrid components of our model include mechanistic models of COTS larval dispersal between reefs, whose predictive influence emphasises the central role of dispersal on COTS irruptions. Further analyses of variable importance support key hypotheses regarding COTS population dynamics, including the roles of chlorophyll and temperature, and the regional benefits of local management. When compared to existing COTS models, our hybrid approach produces more accurate short term forecasts that would improve managers' ability to target high-risk reefs. Along with producing accurate hindcasts, the model shows promise for predicting irruptions during critical periods at the initiation of GBR-scale irruptive events, which the model suggests are underway in 2026.

Keywords: hybrid modelling; irruptive species; pest management; crown-of-thorns starfish; decision support

1 Introduction

Irruptive species exhibit boom-bust dynamics: extreme population increases over short periods of time, sometimes by orders of magnitude within a fraction of an individual's lifespan (Royama 1984; Jiménez et al. 1992; Andersen & Linnell 2000; Mills 2001; Pratchett et al. 2024). Such rapid and severe increases in population can result in major economic losses. For example, locust outbreaks have resulted in over one billion US dollars (2019) in crop damages and management expenditure in the past 25 years (Zhang et al. 2019; Bank 2026), with a single outbreak capable of impacting the food security of over 8 million

people (FAO 2022). Irruptive species can also cause substantial environmental damage when invasive, or when anthropogenic factors exacerbate irruptions and reduce ecosystem resilience. A good illustration is the widespread death of marine species caused by harmful algal blooms (HABs), which have increased in frequency and intensity as a result of pollution (Yan et al. 2024; Zahir et al. 2024).

Producing forecasts of population irruptions is important for effective prevention, suppresssion, and management, especially given comprehensive real-time monitoring is generally infeasible. However, forecasting irruptions is fraught with difficulty due to a number of factors. Of these factors, the most significant is the volatile nature of these irruptive events, the drivers of which are often numerous, nonlinear, and interactive, if understood at all (Wooldridge & Brodie 2015; Ørsted et al. 2021; Yan et al. 2024; Srivastava et al. 2024; Goroshko et al. 2025). Anthropogenic pressures (e.g. global warming) introduce additional complexity by rendering these dynamics and drivers nonstationary, which can lead to changes in population dynamics and distribution (Howe et al. 2024; Srivastava et al. 2024; Al-Wardy et al. 2025). Finally, many irruptive species dynamics are heavily influenced by their ability to spread to nearby habitat, which can be difficult to accurately quantify (Hock et al. 2014; Powell & Bentz 2014; Veran et al. 2015; Li et al. 2020; Stewart et al. 2026).

Early attempts at forecasting irruptions typically take a mechanistic modelling approach (e.g. MacLean et al. 2001; Deveson & Hunter 2002; Silva et al. 2016), often necessitated by limited survey data or predictive variables that preclude the use of statistical or machine learning (ML) methods (Sturtevant et al. 2015; Piou & Marescot 2023; Zahir et al. 2024). Mechanistic models can aid in developing understanding of causal relationships, explicitly incorporate existing knowledge, and conduct scenario analysis by predicting the effects of management. However, the dynamics of irruptive species often require equations with nonlinear components (Sturtevant et al. 2015; Mamo et al. 2025), whose structure and parameters can be difficult to identify which can produce highly sensitive models. Similar issues arise regarding the inclusion of external drivers of population dynamics, each of which must have their effects (including interactions) incorporated by structured and parameterised relationships. It is therefore not certain that these models are sufficiently accurate to forecast the timing, scale, and location of irruptions (Wood & Thomas 1999; Novak et al. 2011; Lubiana Botelho et al. 2025).

If enough precise observations are available, some of these challenges may be alleviated by using traditional statistical models (e.g. Bouchard & Auger 2014; Veran et al. 2015; Vanhatalo et al. 2016), which offer moderate flexibility and strong inferential capability and explainability. Nonetheless, these approaches may still suffer from structural uncertainty and require variable selection, which can inhibit a model's ability to accurately forecast irruptions. Machine learning (ML) models can circumvent these drawbacks given their high flexibility and typically non-parametric nature (e.g. Xiao et al. 2017; Lawton et al. 2022; Srivastava et al. 2024), however require quantities of data that are often prohibitive for ecological systems.

The data requirements of ML approaches can be reduced through hybrid modelling, a technique that integrates established mechanistic relationships into or alongside ML architecture (Von Rueden et al. 2020). Doing so can effectively constrain the optimisation space an ML model is traversing when training, producing better fits with less data. For example, physics-informed neural networks essentially force an ML model to obey physical laws by including them in the loss function (Raissi et al. 2019). This can improve model extrapolation compared to standard ML, offer greater flexibility of application over mechanistic models, and critically, reduce the data required for fitting (Cuomo et al. 2022). Alternatively, hybrid models can involve fitting ML models to the residuals of a mechanistic model to correct them, or can simply include the outputs of a mechanistic model as a predictor in an ML framework (Wesselkamp et al. 2024). Despite their benefits, hybrid models retain a key limitation of their underlying ML architecture, namely a reduced capacity for model interpretability given ML's black-box nature. This can result in issues understanding the drivers of model predictions, making it hard to communicate models to end-users and explore hypotheses.

Hybrid modelling is nonetheless a promising technique for modelling systems with intermediate quantities of data (Yan et al. 2024; Wesselkamp et al. 2024) such as monitored ecosystems. Recently, hybrid modelling has been adopted to model irruptive species, albeit across relatively few studies. For example, Youngblood et al. (2023) predict future locust distributions by including a predictor combining climate projections with mechanistic models of temperature-dependent digestion, which is hypothesised to limit population growth. Similar approaches have also been applied to directly forecast population irruptions on shorter timescales ($<$ 10 years). For instance, Ramazi et al. (2021) produce spatiotemporal forecasts of insect irruptions using a mechanistic model of the species' multiphasic response to low temperatures as a predictor. Other examples

include using mechanistic models of species spread as predictors, such as ocean circulation models for HABs (Baek et al. 2021), and habitat, distance, and human transport corridor dependent dispersal for an invasive beetle species (Shatz et al. 2016).

Crown of thorns starfish (COTS) are an irruptive species whose population dynamics have been modelled mechanistically (Condie et al. 2018; Bozec et al. 2022), statistically (Vanhatalo et al. 2016; Chen et al. 2017), and with machine learning (Islam et al. 2026). COTS cause significant damage to coral reefs including the Great Barrier Reef (GBR), where their predation has repeatedly been identified as a primary driver of coral mortality alongside cyclones and marine heatwaves (Osborne et al. 2011; Sweatman et al. 2011). For example, De'ath et al. (2012) estimated that coral cover on the GBR halved between 1985 and 2012, with 42% of this decline attributed to COTS. The majority of damage from COTS occurs during "outbreaks" – violent population irruptions of up to 6 orders of magnitude in 2 years or less that can cause devastating reductions to coral cover (Birkeland & Lucas 1990; Pratchett et al. 2014; Matthews et al. 2024). As cyclones and heatwaves are predicted to increase in frequency and/or intensity due to climate change (Ainsworth et al. 2016; Cheal et al. 2017; Frölicher et al. 2018; Oliver et al. 2018), their interaction with COTS outbreaks will continue to subject the GBR to a worsening regime of cumulative stressors.

Critically, unlike cyclones and marine heatwaves COTS are currently the only major disturbance that can be managed at a local scale (Pratchett et al. 2014; Vercelloni et al. 2017) through targeted culling. Furthermore, outbreaks can propagate via larval dispersal (Stewart et al. 2026), leading to benefits at not just each reef culled, but also their downstream neighbours (Matthews et al. 2024). Like many conservation programs, COTS culling is heavily resource constrained (GBRMPA 2024a); during the 2023-24 financial year, for example, only 2.3% of the GBR's reefs received culling efforts (GBRMPA 2024b). To ensure that maximum benefit is gained from culling efforts reefs are prioritised based on their economic and ecological value, the latter of which considers the risk of an outbreak occurring (GBRMPA 2024a; Matthews et al. 2026).

Due to the lack of survey data available for the vast majority of reefs, COTS populations are predicted by mathematical models. When selecting reefs for culling, accurate short-term predictions are key as early intervention in outbreaks yield the highest chance at suppressing them and thus producing the best outcomes for coral cover (Matthews et al. 2024). Even if reefs are visited when an outbreak is already underway, the rate at which COTS can be culled increases at higher COTS densities (Fletcher et al. 2021) which may reduce the probability of spread to nearby reefs (Benzie & Dixon 1994; Rogers et al. 2017; Stewart et al. 2026). Finally, correctly identifying reefs with outbreaks can greatly reduce operational costs by minimising the time spent travelling between reefs without problematic population densities.

Despite the existence of many COTS population models, only two operate at a spatiotemporal scale and accuracy levels appropriate for guiding yearly COTS culling resource allocation. The first is a mechanistic model (Bozec et al. 2022), which despite its complexity and ongoing development reports low precision (0.4) for identifying outbreaks during periods in which they are widespread (2008-2022, Skinner et al. 2024). The second is an ML model with a simple hybrid component that predicts a reef's long-term risk of experiencing an outbreak (Matthews et al. 2020a). To account for the strong temporal dynamics in COTS populations (Figure 1, Moran et al. 1992; Pratchett et al. 2014, 2024), this model has since been adjusted to map the distribution of recently observed outbreaks in 2 year increments (Matthews et al. 2026). However, this does not explicitly forecast outbreaks, and due to the model's temporally-static predictor set restricts training data to a 2-year period, constraining its accuracy.

The lack of an explicit and accurate forecasting tool for COTS outbreaks hinders COTS management decision-making. In this paper, we address this limitation by developing the first hybrid ML outbreak forecasting model. Utilising the temporally-static predictor set from Matthews et al. (2020a), we build a new model that includes numerous additional predictors that capture both the recent and historical conditions on each reef. The hybrid component of our model involves simulating the process of COTS reproduction and spread to nearby reefs, using mechanistic models that combine physics-based simulations of ocean currents with individual-based models of larval biology (Choukroun et al. 2025; Stewart et al. 2026). We compare our hybrid model's performance to alternatives in predicting future outbreaks, recovering historical dynamics at unsampled reefs, and guiding COTS management decision-making.

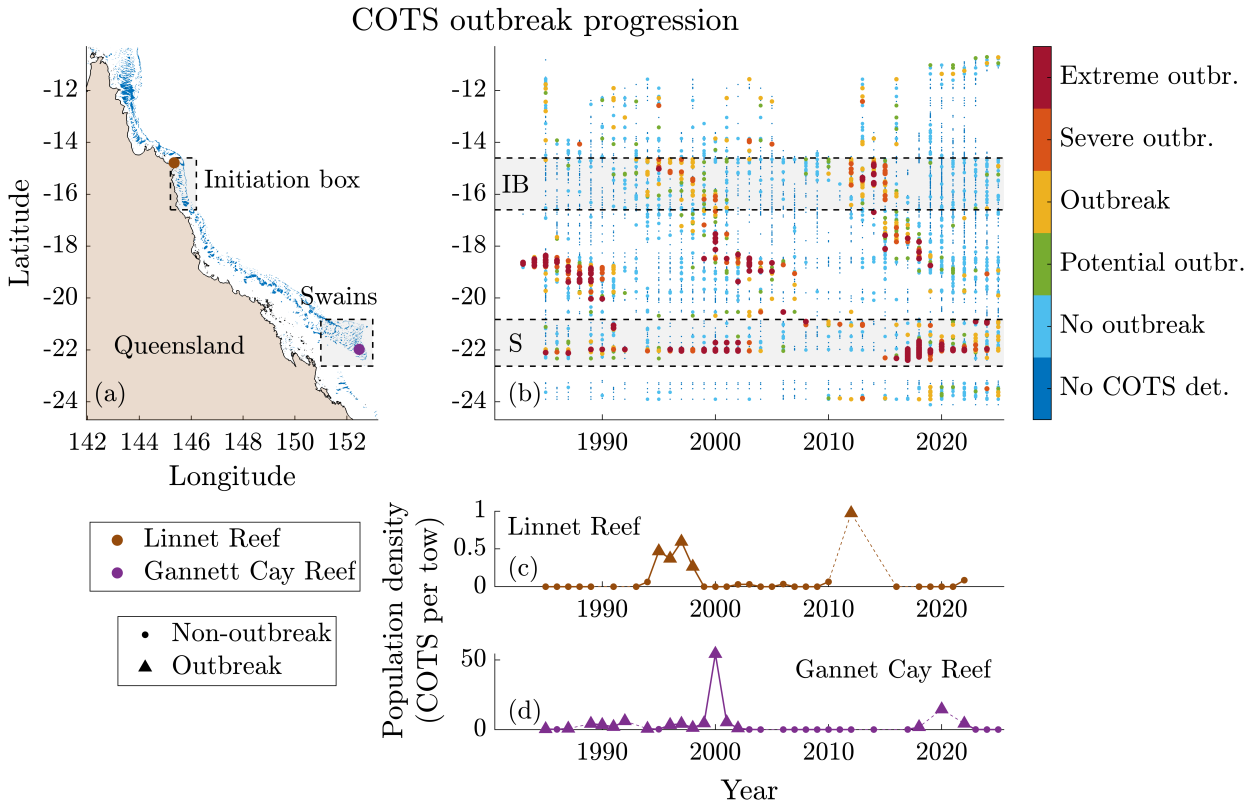

Figure 1: Diagram (a) highlighting key areas for COTS outbreaks, and (b) the history of COTS population density across the GBR. Data consists of manta tow surveys conducted by the Australian Institute of Marine Science's Long-Term Monitoring Program, Queensland Parks and Wildlife Service's Joint Field Management Program, and the Great Barrier Reef Marine Park Authority's COTS Control Program. Each point in (b) represent an observation of COTS density for a single reef in a single year, with densities converted into 6 distinct categories following Skinner et al. (2024) as indicated by both colour and size. These are defined in units COTS per tow, and consist of: No COTS detected = 0, No outbreak $\in (0, 0.11]$, Potential outbreak $\in (0.11, 0.22]$, Outbreak $\in (0.22, 1]$, Severe outbreak $\in (1, 3]$, Extreme > 3.0. Examples of COTS population density dynamics are included for (c) Linnet Reef in the initiation box, and (d) Gannet Cay Reef in the Swains, with dotted lines indicating years without observations.

2 Methods

Our overall goal was to produce forecasts that can improve COTS control efforts. Since these are allocated yearly, at the scale of individual reefs, we developed a model capable of predicting the probability that a given reef will experience an outbreak one year in advance. As COTS spawn across December-January (Pratchett et al. 2017a; Caballes et al. 2021), we use calendar years for prediction. In the sections that follow, we describe the process of model development, training, and evaluation.

However, in some circumstances predicting lower COTS densities may prove advantageous from a management perspective. We therefore also train an alternative model that predicts whether a reef will exceed the ecological threshold, which represents a lower COTS density than an outbreak. As this alternative model is almost identical to the outbreak model, we focus on the outbreak model in the main text and discuss the alternative model in Section S5 of the Supplementary materials.

2.1 Background

Study area

The GBR is the most extensive coral reef system in the world, consisting of approximately 3,861 reefs and covering an area of 344,400 km^2 teeming with biodiversity levels equivalent to rainforests (Reaka-Kudla et al. 1997; Small et al. 1998; Borthwick et al. 2006; Plaisance et al. 2011). The GBR provides numerous ecosystem services, from supporting well-known industries like tourism and fishing, to more obscure functions like wave-disruption during cyclones (Young & Hardy 1993; Stoeckl et al. 2011; O'Mahoney et al. 2017). These benefits are not only significant economically, with the GBR contributing $6.4 billion to the Australian economy (O'Mahoney et al. 2017), but also culturally, evident in its designation as a World Heritage Site (UNESCO 2024).

Terminology

The most spatiotemporally-extensive data on COTS populations is collected via manta tow, a sampling procedure that involves towing an observer behind a boat at a standardised speed for a set duration (Miller et al. 2019). When repeated and averaged across a reef's perimeter, manta tows provide estimates of COTS population density in units COTS per tow, a measure used frequently in COTS monitoring, management, and modelling (Fletcher et al. 2020; Matthews et al. 2020b, 2024; Skinner et al. 2024). In this study, we use the standard COTS outbreak definition, where a reef is classified as having an outbreak if it possesses a COTS density above 0.22 COTS per tow. Manta tow surveys can also estimate the precentage of reef covered by hard coral, referred to as coral cover.

COTS outbreaks at individual reefs can broadly be categorised into "primary" and "secondary" outbreaks. Primary outbreaks involve a buildup of COTS that appear to originate independently of other outbreaks, whereas secondary outbreaks appear to have spread from the former (Pratchett et al. 2014). COTS (and their associated outbreaks) spread between reefs via larval dispersal, in which larvae are transported to downstream reefs by ocean currents.

Primary outbreaks are thought to occur within a region in the northern GBR known as the "initation box" (Johnson 1992; Moran et al. 1992; Wooldridge & Brodie 2015), along with the southern Swains region as pictured in Figure 1 (a). The initiation box is a key focus of COTS research and management, as outbreaks formed in this area are followed by outbreak "waves": groups of secondary outbreaks that spread south as a united wavefront across the central GBR, as shown in Figure 1 (b). Historically these waves occur every 15-20 years, however there has been limited sampling on reefs to the north of the initiation box which hinders further investigation into their initiation and propagation.

2.2 COTS population observations

We train our hybrid ML model on the outbreak status of each reef in a given year based on COTS survey data visualised in Figure 1 (for further details, see Section S1 of the Supplementary materials). This data is provided by multiple sources, including the Australian Institute of Marine Science's (AIMS) Long Term Monitoring Program (LTMP) and Queensland Parks and Wildlife Services Joint Field Management Program (JFMP). The LTMP is a large-scale survey effort aimed at monitoring the health and trajectory of the GBR (AIMS 2025). For each year in the program's 35+ year lifespan, between 80 and 130 reefs are surveyed by manta tow across various environmental gradients across the length and width of the GBR. When combined with surveys from the JFMP, the LTMP dataset consists of 3267 averaged manta tows at a reef and year scale, from 1983 to 2025. These surveys are complimented by the COTS Control Program (CCP), who conduct large-scale COTS culling operations across the length of the GBR. This involves surveillance via manta tow, which forms a dataset of 2131 reef-year scale observations from 2012 to 2025, along with data detailing the number of COTS culled across four size classes for each reef.

2.3 Predictors

Our model takes into account almost 100 different predictors, including environmental conditions, spatial location, observed coral and COTS dynamics, and disturbances. Key predictors are summarised in the sections that follow, with all predictors listed in Appendices A and B accompanied by comprehensive descriptions in Section S2 of the Supplementary materials.

2.3.1 Static predictors

The static properties of each reef may influence its susceptibility to outbreaks. For example, a reef's distance to the mainland (i.e. shelf position) has been linked to adult COTS abundance (Vanhatalo et al. 2016), and the abundance of coralline algae positively associated with COTS settlement (Fabricius & De'ath 2001). Similarly, depth can influence coral assemblages (Sheppard 1982; Roberts et al. 2015), exposure to disturbances (Massel & Done 1993), and coralline algae abundance (Johnson et al. 1991; Doll et al. 2023), and has been linked to COTS settlement (Wilmes et al. 2020). We also include summary statistic of each reef's long-term COTS density and coral cover as static predictors, which are calculated for reefs with 2 or more years of manta tow surveys. However, as only 15% of reefs on the GBR have received 2 or more years of surveys, we include imputations of these long-term summary statistics using a spatial averaging technique tuned separately for each statistic.

2.3.2 Dynamic predictors

Hybrid predictors

Given the dynamic nature of outbreaks we also consider multiple predictors that capture relevant conditions for each of the 6 preceding years to the year being predicted. For example, the process of COTS reproduction is thought to be a key driver of outbreaks (Hock et al. 2014; Matthews et al. 2020a; Stewart et al. 2026), and we therefore include predictors derived from mechanistic modelling of COTS reproduction. This model of COTS reproduction constitutes the hybrid aspect of our model, and utilises models of COTS dispersal presented in Choukroun et al. (2025) and Stewart et al. (2026). These dispersal models first draw upon hydrodynamic models, which apply physical laws and forcings to resolve fine-scale ocean currents across the entire GBR. Individual-based larval simulations are then placed within these current fields to simulate millions of dispersal trajectories for each COTS spawning season, creating networks of potential connections between reefs. These simulations incorporate key biological processes, particularly stochastic age-based maturity and mortality rates. Uncertainty and temporal variability in key processes is addressed through an ensemble modelling process that averages dispersal dynamics across 1,344 different dispersal networks (Stewart et al. 2026).

The process of simulating COTS reproduction using these dispersal predictions is detailed in Figure 2. First, COTS densities are imputed at unsampled reefs with spatial averaging and machine learning, before using these densities to compute the quantity of larvae produced at each reef. Without this imputation step the amount of larvae produced in a region would be directly tied to surveillance effort, which varies in time and space (Figure 1b). Larvae are then distributed across the GBR using the aforementioned COTS dispersal predictions, providing an estimate of the density of larvae settling at each reef during each year that we refer to as the connectivity autocovariate:

$$\tilde{C}_{r,t,t_b} = \frac{1}{a_r} \sum_{m \in R} a_m p_{m,t-t_b} c_{m,r} \quad \text{if} \sum_{m \in R} c_{m,r} a_m \geq 0.9 \sum_{m=1}^{N} c_{m,r} a_m, \quad t_b \in \{1, ..., 6\}, \tag{1}$$

where $\tilde{C}_{r,t,t_b}$ is the connectivity autocovariate for reef r, t_b years before the current year t. The number of reefs in the GBR is denoted N, with the mth reef possessing a COTS density of $p_{m,t-t_b}$ for year $t - t_b$, which is imputed if the reef was not surveyed. Here, we compute a reef's larval production using each reef's perimeter a_m rather than area, as the majority of COTS habitat exists around the reef perimeter. We denote the connectivity strength from reef m to reef r with $c_{m,r}$, which corresponds to the probability that a larva produced at reef m will successfully settle at reef r. Finally, R is the set of reefs for which COTS density can be imputed or observed.

We ensure that the connectivity autocovariate is only calculated for reefs that have a sufficient number of source reefs with imputed or observed density values $p_{m,t-t_b}$. This avoids underestimating the amount of incoming larvae in undersampled regions, which would undermine the model's ability to fit the data effectively. To do so we calculate the potential larval income (Equation 1), which we define as the estimated quantity of larvae arriving at a reef if all reefs are assumed to have a uniform density of 1 COTS per tow. Reef-year pairs for which $> 10\%$ of their potential larval income is sourced from reefs without imputed density values are then assigned a missing value NA to $\tilde{C}_{r,t,t_b}$. These missing values can be handled by the

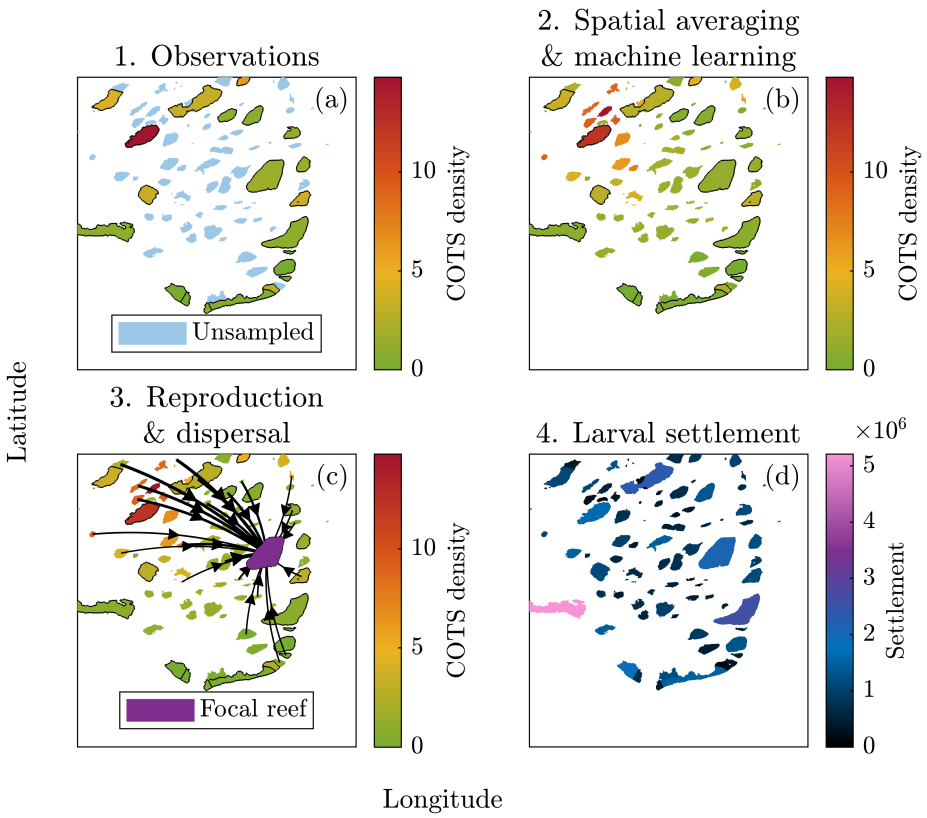

Figure 2: Diagrammatic representation of the connectivity autocovariate, which simulates COTS reproduction. Panel (a) demonstrates spatial gaps in surveyed reefs with those coloured blue being unsurveyed, (b) whose COTS populations are then estimated using a mix of spatial averaging and machine learning. Panel (c) represents the process of reproduction and subsequent larval dispersal to a single reef (purple) for visual clarity, which (d) when repeated allows for the estimation of the amount of larvae settling at all reefs.

boosted regression tree ML architecture we utilise (XGboost, see Section 2.4), by assigning missing values to either side of binary splits inside each decision tree.

Our goal in adding this hybrid component is to improve model accuracy using the limited survey data available. In theory, as the quality and quantity of data increases, the flexibility of ML models would allow them to accurately infer complicated relationships. In practice, this is seldom possible: for COTS, this would require inferring – without guidance – the strengths of almost 15 million larval connections between reefs, yearly COTS densities at 3861 reefs, and the relationship between COTS density, reef size, and reproductive output. Despite an imperfect and incomplete understanding of these processes, specifying them explicitly using up-to-date mechanistic knowledge can greatly reduce the data required for a given level of model accuracy. Furthermore, uncertainty in these processes can also be reduced by trialling competing relationships, and selecting the approach that performs best using cross-validation. For example, we trialled several relationships between COTS density and reproductive output, and selected the best performing relationship (linear) with holdout validation (validation set, see Section 2.5.1).

Non-hybrid predictors

COTS reproduction is thought to be influenced by the conditions larvae are exposed to while in their dispersal phase. We therefore include satellite measurements of Chlorophyll-*a* (NASA 2025), as phytoplankton levels have been hypothesised to take a central role in the formation of outbreaks (Birkeland 1982; Lucas 1982; Brodie et al. 2005; Fabricius et al. 2010; Wooldridge & Brodie 2015). We also include satellite-derived Sea Surface Temperature (SST, NOAA 2025b), as both temperature and Chlorophyll-*a* levels have been

shown to influence larval development and survivorship (Wolfe et al. 2015; Caballes et al. 2017b; Kamya et al. 2014; Lamare et al. 2014; Pratchett et al. 2017b; Uthicke et al. 2018). Both SST and Chlorophyll are averaged over the COTS spawning season and pelagic larval duration (Pratchett et al. 2017b; Caballes et al. 2021) and within a 110km radius of each reef, as the COTS dispersal models detailed above predict 90% of larvae settle within 110km (Stewart et al. 2026). Additionally, we include predictors related to coral as they represent the primary food source for COTS. These include the maximum Degree Heating Weeks experienced at each reef, as heat stress leads to coral bleaching and mortality (Hughes et al. 2017) and has been linked to COTS detection (Cook et al. 2026). We also model the impact of cyclones (De'ath et al. 2012) following Edwards et al. (2011) using cyclone position and strength data provided by BoM (2025).

Given the observed impact of COTS control at both a reef and regional level (Matthews et al. 2024), we include predictors based on the number of COTS culled at both the reef itself, and all reefs within a 110km radius. We also derive dynamic predictors from manta tow observations of COTS and coral populations. Specifically, we infer recent COTS and coral populations at each reef, estimated tuned spatial averaging algorithm. When applying these spatial averaging techniques, reefs that have received culling effort in the past 5 years are excluded, given their populations will not be representative of their neighbours that aren't culled. That is, culling COTS reduces their abundance and hence their predation on coral populations, thus altering dynamics compared to reefs without culling effort.

2.4 Model training

Following standard ML practices, we split our observed COTS data into three subsets for model training, validation, and testing. These splits are determined by year to resemble the primary use case for our model: forecasting into an uncertain future. First, the training set is used to fit the model, and contains 2422 COTS observations between 1991 and 2017 inclusive. Model parameters can then be calibrated using the validation set, which consists of 736 observations spanning 2018 to 2020 inclusive. Finally, the model's performance on unseen data is estimated using the testing set, which encompasses 1251 observations between 2021 and 2025 inclusive.

The ML architecture we apply is a boosted regression tree (BRT) model, which involves fitting an ensemble of decision trees. Each decision tree is formed by conducting a number of binary splits on predictors, each split aiming to improve model accuracy by minimising a loss function specified by the modeller. While each individual tree is simple they are fit sequentially to the errors of all preceding trees, allowing the model to capture complex relationships. The specific properties of model – for example the complexity of each tree – are referred to as hyperparameters, and can be specified by the modeller.

Our model is trained using the package "xgboost" (Chen et al. 2015) for R, which fits a variant of BRTs. Compared to standard BRTs, xgboost offers improvements to computational efficiency, can automatically accommodate missing data, and integrates regularisation into the fitting process. To train our model, we use a weighted variant of the binary cross-entropy (log-loss) as our loss function ℓ, which the model aims to minimise:

$$\ell = -\frac{1}{B}\sum_{i=1}^{B} w_i \left(y_i \log(\hat{y}_i) + (1 - y_i)\log(1 - \hat{y}_i)\right) \tag{2}$$

where y_i is the ith observation out of B total, with $y_i = 1$ indicating an outbreak and $y_i = 0$ a non-outbreak. The response is $\hat{y}_i$, representing the predicted probability that the ith observation is an outbreak. The weightings w_i account for the class imbalance within our training and validation sets, in which only 14% of observations are outbreaks. Using the validation set, we determined a weight of $w_i = 50$ for outbreaks and $w_i = 1$ for non-outbreaks leads to optimal model accuracy across both classes. Hyperparameters were selected using the same approach, aside from the number of trees which was determined using 10-fold cross validation on the training data (see Section S1, Supplementary materials).

When examining predictions from the model, it was noted that the model consistently underestimated the proportion of outbreaks across the GBR when applying a probability cutoff of 0.5 for binary classification. We therefore tuned the probability cutoff using both the training and validation datasets. This involved producing predictions for each year from 1991 to 2020, each time training the model on all training and validation data aside from the year being predicted and the four years following. By varying the cutoff in

0.05 increments, it was determined that a cutoff of 0.45 minimised the mean yearly outbreak underpredictions. Due to this change in framing of outputs, we hereafter refer to the model outputs as outbreak potential rather than probability, aside from cases where binary classification is being discussed.

2.5 Model evaluation

2.5.1 Evaluation scenarios

Once the predictors have been formed the model has been trained, its performance can be evaluated. While the model is primarily designed for use in the CCP's prioritisation process (Matthews et al. 2026), there are multiple additional use-cases that we accommodate for. As such, we assess model accuracy using several different partitions of our COTS survey data, which are detailed below.

Test set accuracy

An important metric of model accuracy is its performance when applied to the testing set, as this represents an estimate of its performance on unseen data. When making predictions on the testing set, the model is retrained on all data up until the year being predicted, to mimic the intended use-case for the model. This same training approach is also used for the validation and primary outbreak sets, described below.

Validation set accuracy

Despite being an important tool for measuring model performance, our testing dataset falls upon a window of time at which observed COTS outbreaks are at a relatively low level (Figure S2). To instead investigate model performance during an outbreak wave, we also present the performance of our model when applied to the validation set, which covers the tail end of an outbreak wave (Figure 1b).

Hindcasting

Another potential use of the model involves estimating historical outbreak dynamics at unsampled reefs, which may lead to a better understanding of historical COTS dynamics. To do so, we split all the sampled reefs in our dataset (including the validation and testing sets) into 90% for fitting, and 10% for evaluation. Survey data from the reefs in the evaluation dataset are not used to form or impute recent or historical predictors regarding coral cover and COTS, including for the evaluation reefs themselves. As such, this evaluation set represents reefs the model has never trained on, and whose specific set of properties it may not have encountered.

Additionally, we produce GBR-wide hindcasts from 1991 to 2025, to ensure that hindcasts can capture broad COTS population dynamics. When doing so, we aggregate both observations and hindcasts for each degree of latitude, to facilitate a comparison between the two. Observational data is included for latitudinal degrees with 3 or more observations. These observations are sourced from both the routine surveys (LTMP etc.) and the CCP, the latter of which may contain upwardly-biased estimates of outbreak prevalence given reefs are selected in part based on their estimated COTS population. Even routine surveys may contain spatial biases, for example the lack of effort on the inner and outer shelf in some regions (see Figure S1, Supplementary methods) that naturally sustain less outbreaks, which is concealed when aggregating over latitude. As such, we are more concerned with whether hindcasts exhibit similar spatiotemporal patterns of outbreak dynamics to surveillance data, rather than matching the exact magnitudes of outbreak prevalence. To account for these issues, we also make comparisons to observations regarding spatial patterns when hindcasts are averaged through time, and temporal dynamics when average across space. Doing so assesses the model's ability to capture GBR-wide outbreak wave cycles, and identify reefs (and regions) with historically high outbreak risk.

Primary outbreak detection

COTS outbreaks at individual reefs can be categorised into primary outbreaks, that appear to arise independently, and secondary outbreaks that follow from either primary or other secondary outbreaks. It is hypothesised that primary outbreaks forming in the initiation box lead to outbreak waves, which spread south through the GBR over a 15-20 year period. Predicting primary outbreaks in the initiation box is

therefore critical to effective COTS management, given early intervention may have the potential to alter the trajectory of the resulting outbreak wave (Babcock et al. 2020). We therefore assess the model's ability to identify primary outbreaks, by evaluating the model's predictive accuracy from 1992 to 1994 in the Cairns-Cooktown region/initiation box (between the latitudes -16.5° and -14.5°, containing 256 reefs). This period contains 73 reef-year surveys with 10 representing outbreaks, including one year before the first outbreaks are detected.

Since 2019, data from fine-scale survey methods including SALAD surveys and eDNA have documented increases in COTS densities in the initiation box (Chandler et al. 2023; Uthicke et al. 2024), suggesting the beginning of a new outbreak wave. Despite their improved precision (Pratchett et al. 2022, 2026) these methods cover a far smaller spatiotemporal extent than the manta tow data used to train our model, and currently lack a method for conversion (Lawrence et al. 2026). Nonetheless, this independent data can be used to further evaluate our model's efficacy during the emergence of primary outbreaks in a qualitative manner. To do so, we train the model on all available data (1991-2025, inclusive), and produce predictions across the GBR for 2026. We use these predictions to identify the reefs with the highest outbreak potential, and examine changes in outbreak potential between 2024 and 2026. We note here that at the time these predictions for 2026 were produced, the authors had not accessed nor seen any COTS surveillance data from 2026.

2.5.2 Comparative models

In order to contextualise our model we compare its performance to a number of alternatives. The first and most simple is to prioritise reefs completely at random, serving as a baseline scenario. Clearly however, COTS managers do have prior information they may choose to draw upon, namely surveillance data. We therefore apply an alternative baseline in which reefs are prioritised in descending order by their most recently observed COTS density (by manta tow) in the two preceding years.

In practice, the COTS outbreak model introduced in Matthews et al. (2020a) is used to estimate COTS outbreak risk in COTS control prioritisation (Matthews et al. 2026). This model uses an ML architecture with a hybrid component to approximate COTS reproduction, similar to our approach described in Section 2.3.2. Comparatively, however, it is a simpler implementation: COTS densities are not estimated at unsurveyed reefs, are converted to a binary 0 for non-outbreak and 1 for outbreak, and the size of the source and sink reefs are not considered. We compare our model to two versions of the Matthews model: the original version which we refer to as simple hybrid (long-term) that estimates long-term outbreak risk, and the adjusted version we term simple hybrid (recent) that aims to capture the recent distribution of outbreaks. This adjusted version also includes COTS culling data in its training process, which is further described in Section S3 of the Supplementary material. Additionally, both models have been updated by replacing the previous estimates of COTS dispersal dynamics (Hock et al. 2014, 2017) with new results produced by Stewart et al. (2026).

We provide two approximate comparisons of our model's performance to the leading mechanistic model for both coral and COTS abundance predictions on the GBR (ReefMod, Bozec et al. 2022) as described in Skinner et al. (2024). These results span COTS observations from 2008 to 2022, and as such comparisons are conducted separately to the datasets detailed in Section 2.5.1. Additionally, given the COTS density predictions presented in Skinner et al. (2024) are converted into and reported as 6 abundance categories, only 5 point estimates are available for some of our comparisons. For the first version of our comparison to the mechanistic model, we train our model on all data up until the year predicted, as well as data from 2023 onwards. However, doing so puts our hybrid ML model at a significant disadvantage, given the model is trained on just over 2000 observations at the start of the comparison period. One of the primary reasons a dynamic ML model had not been previously explored is the lack of data, given machine learning approaches rely on large datasets to learn complex relationships. We therefore also provide a second comparison, in which 90% of the data between 2008 and 2022 is included in the model's training set, and 10% is used for testing. In contrast, this comparison provides our model with an unfair advantage, given the model is able to train on future conditions; we hypothesise the actual model performance would sit between these two extremes.

2.5.3 Improving model prediction at undersampled reefs

The goal of irruptive species modelling is often to complement surveillance data, by either predicting irruptions into the future or on sites that have been insufficiently surveyed. Modelling COTS is no different, however the dynamics of COTS populations and the manner in which they're surveyed requires additional consideration. COTS populations at individual reefs exhibit strong autocorrelation: a reef in a non-outbreaking state is unlikely to experience an outbreak the following year. If a reef does transition to on outbreaking state, it will typically last 3-5 years (Figure 1c), or longer in the Swains region (Figure 1d). Knowing the recent status of a reef therefore provides a substantial boost in predictive power. However, the majority of reefs on the GBR are not surveyed frequently by manta tow, with ≈80% of reefs lacking any survey data. In contrast, reefs that are surveyed have often been visited multiple times, and it is these reefs that form the majority of data used to train and evaluate our model. For example, only 15% of reefs on the GBR have received 2 or more years of surveys, compared to 70% of reefs used for training and evaluating our model. As such, models that rely too heavily on surveillance data may appear to perform well when evaluated, but in reality perform poorly at the undersurveyed reefs for which their predictions are more valuable.

We account for the biased distribution of surveillance effort in both the formation of our model's predictors, and our process for model evaluation and comparison. Regarding predictors, when using spatial averaging to estimate the recent COTS and coral populations at each reef, survey data from the reef itself is excluded. We also only provide the model with 25% of long-term COTS and coral population summary statistics and 60% of their estimated counterparts, both proportions determined using holdout validation. These changes only apply during model training and evaluation: in practice, when producing GBR-wide forecasts or hindcasts to guide management all survey-based and estimated summary statistics are utilised. This allows the model to utilise additional information when it is present, while avoiding an overdependence on data that is not available for the vast majority of reefs.

The distribution of surveillance effort should also be accounted for when assessing a model's utility for guiding conservation effort, which is evident in the most recent evaluation of the mechanistic COTS model's performance (Skinner et al. 2024). In this study, after accuracy for a given year is assessed, modelled COTS populations are then reassigned to observed values where available. When later analysing factors that impact model accuracy, Skinner et al. identify that accuracy decreases as the years since a survey at a reef increases, and as the total number of surveys decreases. This makes sense given autocorrelation in COTS population data, and the fact that during the testing period (2008-2022) many surveyed reefs were also surveyed in the preceding year (≈40%) or within the preceding 3 years (≈70%). The accuracy reported by Skinner et al. (2024) is therefore not representative of the model's performance across the majority of the GBR which receives little to no surveillance, and instead represents an upper bound on accuracy.

Similar issues could arise for the simple hybrid model (recent), as a consequence of two interacting factors. The first is that ML models often fit extremely well to their training data, and the second that the predictors in the simple hybrid model (recent) remain the exact same when training and forecasting. As such, these close fits to training data are then replicated when predicting onto a testing year for any reef that appears in both sets. Given the aforementioned autocorrelation in COTS populations and bias in surveillance effort, this would conflate model performance with autocorrelation. We circumvent this issue using a process similar to k-fold cross validation, in which any reefs that both appear in the current year's testing data and were observed in the 2 years prior are placed randomly into 20 folds (or the number of reefs identified if < 20). Each time the reefs in a specific fold are predicted, reefs in the same fold were removed from the training data, avoiding the issue described above. This approach is applied for both our hybrid model and the simple hybrid model (recent) when during model evaluation on the testing, validation, hindcasting, and primary outbreak datasets.

2.5.4 Evaluation metrics

The most relevant evaluation of model performance involves directly simulating its effectiveness at guiding COTS control operations. Specifically, we simulate visiting reefs in order of their predicted risk of an outbreak, and record the cumulative proportion of visits with outbreaks. Uncertainty is quantified by treating the cumulative proportion of outbreaking reefs as a binomial proportion, and computing the associated 95% confidence interval. As we visit reefs based predicted outbreak risk, we ignore the other economic and

ecological factors that guide COTS Control for ease of interpretation and comparison. When doing so, we account for the difference in the number of observations in each evaluation scenario by scaling the total number of observations to the total number of reefs across the GBR, 3861. This grounds results in a practical context, allowing for the examination of model performance at 100 and 200 reefs, approximately the number of reefs controlled and surveyed each year, respectively (GBRMPA 2024b). The exception is primary outbreak detection, which is scaled to a total of 256 reefs to match the number of reefs in the initiation box region.

Additionally, we consider the spatial coverage of each comparative model, and scale results accordingly. This accounts for the fact that despite the potential to provide more accurate results, using observations to guide prioritisation is heavily limited by the number of observations available. Similarly, the simple hybrid (long-term) model can only form predictions for approximately 50% of the reefs on the GBR, whereas our hybrid model covers all reefs.

These prioritisation simulations are supplemented by two standard evaluation techniques for binary classification models. The first technique involves computing the area under the curve (AUC) of receiver operating characteristic (ROC) curves, for each of the model evaluation and comparison datasets. The AUC represents the probability that a randomly selected positive observation (observed outbreak) has a higher predicted probability than a randomly selected negative observation (observed non-outbreak). As such, an AUC value of 0.5 indicates the model is no better than random chance, and 1 indicates the model is always correct. We also use AUC to determine whether there are regional differences in model performance. We do so by producing predictions for each year from 1991 to 2025, each time training the model on all data aside from the year being predicted and the four following years. The model's AUC was then computed separately for each of the 11 LTMP sectors that span the GBR. Finally, we produce confusion matrices by classifying reefs as outbreaking if their outbreak potential exceeds 0.45, and non-outbreaking otherwise. These confusion matrices are a coarse representation of model performance, consisting of only a single point on the aforementioned prioritisation simulations and ROC curves.

2.5.5 Model explainability

A significant limitation of hybrid models is their limited ability for inference and explainability, both of which can vary across both the specific hybrid model setup and its underlying ML architecture. For example, our model's BRT architecture can provide estimates of each predictor's influence during the fitting process, albeit without elucidating the shape of the relationship. For our case study, we're interested specifically in whether key drivers of our model's predictions align with leading hypotheses regarding COTS population dynamics. To examine drivers of model predictions we plot the "gain" for each predictor, which corresponds to its normalised contribution to model training accuracy. Larger values of gain indicate a higher contribution to training accuracy, implying a greater influence on model predictions. When doing so, we aggregate predictors representing the same quantity across different years for clarity.

3 Results

3.1 Prioritisation simulations

Figure 3 presents the performance of models when the process of prioritisation is simulated. It should be noted that the performance across datasets should not be directly compared, given the difference in the proportion of observed outbreaks in each datasets (e.g. 4% in the testing set vs 14% in validation). Additionally, the validation set was used to tweak our model's parameters, and will thus overestimate the model's performance. Nonetheless, across all four datasets our outbreak model outperforms all alternatives, sometimes by a significant margin. For example, on the independent testing set 38 of the first 100 reefs visited would contain outbreaks if our hybrid model was used, compared to the next best approach, simple hybrid (recent), that achieves 15. This pattern is consistent across most datasets, with our model consistently delivering an 1.25 to 2-fold improvements in accuracy at 100 and 200 reefs visited comparative to the next best performing approach. The exception is the validation dataset, for which our model offers only moderate improvements, performing similarly to the simple hybrid (recent) model for the first 200 reefs visited. Our

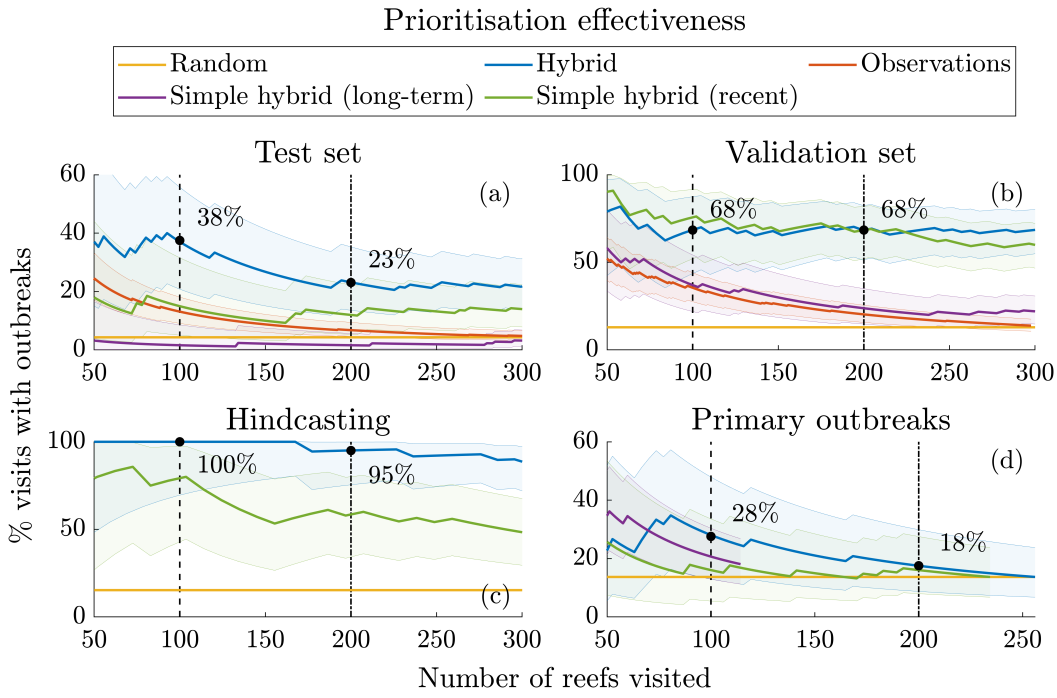

Figure 3: Results of simulating COTS control prioritisation across different decision-making approaches and scenarios. This includes our hybrid model's performance when applied to (a) the independent testing set, (b) the validation set, (c) hindcasting, and (d) primary outbreak detection (see Section 2.5.1 for further details). Model performance is compared to outcomes achieved if reefs were visited randomly, and if reefs were visited in order of the most recently observed COTS density within the previous 2 years. Performance is also compared to a simple hybrid model presented in Matthews et al. (2020a) (long-term), and an adjusted version of the model trained on only the past 2 years of survey data (recent). Due to high levels of uncertainty, we exclude the first 50 reefs visited from our visualisation.

model also performs particularly well at hindcasting, with all of the first 160 reefs visited experiencing outbreaks.

3.2 ROC curves

As ROC curves don't consider the number of reefs each model can form predictions for, Table 1 demonstrates a different order of model performance compared to prioritisation simulations. Our model exceeds an AUC of 0.75 in all cases, performing similarly to the observations-based approach, aside from the primary outbreak dataset in which the latter offers a significant improvement. Compared to both simple hybrid models, our approach offers improved accuracy across all datasets. Additionally, our model achieves an AUC of 0.86 for the hindcasting dataset, again highlighting its ability to accurately predict past outbreak dynamics on unsampled reefs. When examining accuracy at a regional scale, we find that for the majority of the GBR the AUC values sit between 0.75 and 0.9 (Figure S8, Supplementary material). The exception is the decrease in the most northern and southern regions to 0.65, which have substantially fewer observations (Figure S9, Supplementary material).

3.3 Confusion matrices

The confusion matrices in Figure 4 demonstrate reasonable accuracy across the 4 datasets when considering the difficulty surrounding COTS outbreak prediction. For both the validation and hindcasting datasets, the model's true positive rate and precision both exceed 0.5. This indicates that the majority of truly outbreaking reefs would be correctly identified by the model, and that the majority of reefs predicted to

Table 1: Area under the receiver operating characteristic curve (ROC) for each model and dataset. Full ROC curves are presented in the Supplementary material, Figure S7.

	Area under receiver operator characteristic curve			
Dataset	Hybrid	Simple hybrid (recent)	Simple hybrid (long-term)	Observations
Testing	0.79	0.71	0.59	0.83
Validation	0.91	0.86	0.7	0.88
Hindcasting	0.86	0.72	NA	NA
Primary	0.76	0.62	0.78	0.89

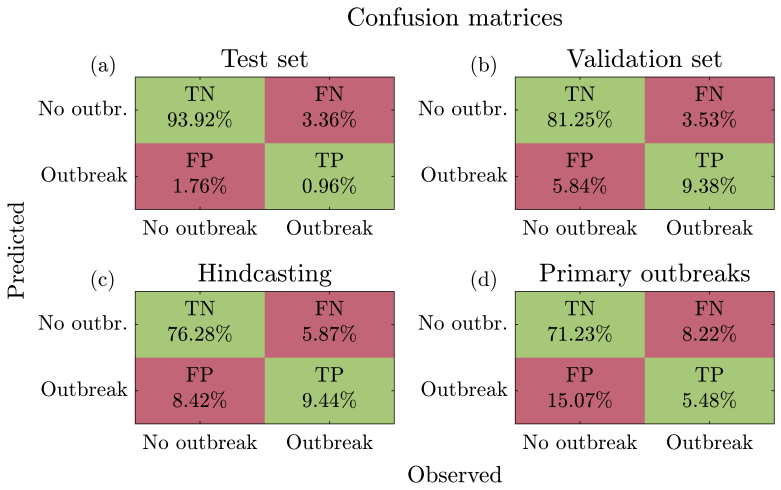

Figure 4: Confusion matrices for our hybrid model's performance when applied to (a) the independent testing set (n = 1251), (b) the validation set (n = 736), (c) hindcasting (n = 392), and (d) primary outbreak detection (n = 73, see Section 2.5.1 for further details). TP = true positive, FN = false negative, FP = false positive, and TP = true positive.

be outbreaking would be outbreaking. This is not the case however for the testing and primary outbreak datasets, which both report a true positive rate and precision less than 0.5. In contrast, the vast majority of reefs that are truly non-outbreaking are correctly classified across all datasets.

3.4 Mechanistic model comparison

Figure 5 demonstrates that our hybrid model outperforms the mechanistic model for guiding COTS control prioritisation for both versions of our approximate comparison. For the first comparison (C1) in which our hybrid model is at a disadvantage, the confusion matrices, ROC curves, and prioritisation simulations report only a minor improvement in accuracy. However, when examining the second version of this comparison our model produces significantly more accurate predictions of COTS outbreaks across all evaluation techniques.

3.5 GBR-wide hindcasts

Figure 6 shows that GBR-wide hindcasts recover broad spatiotemporal features of COTS outbreak dynamics consistent with survey data, while extending predictions to reef/year combinations that were not observed. The model's predicted proportion of outbreaks captures the southward progression of outbreak waves originating in the initiation box, recurrent outbreaks in the Swains region, and the lulls in outbreaks between both of these events. Figure S10 (Supplementary materials) further demonstrate the model's ability to repli-

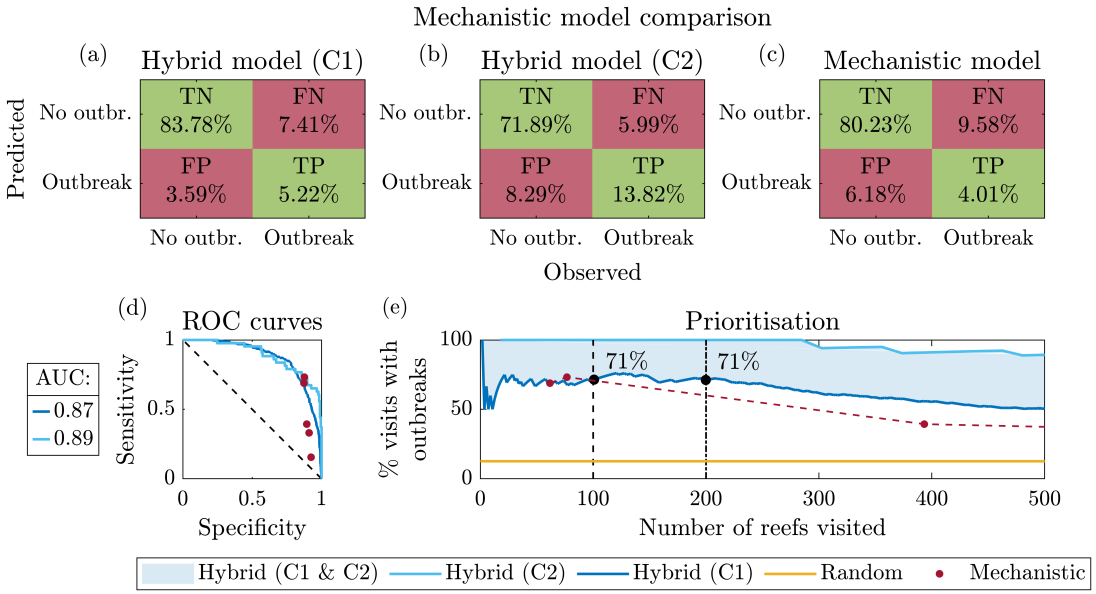

Figure 5: Results of the approximate comparisons between our hybrid model and the leading mechanistic model (ReefMod) on COTS survey data collected between 2008 and 2022 as detailed in Skinner et al. (2024). The suffixes "(C1)" and "(C2)" correspond to the first and second versions of this approximate comparison, respectively. In the first comparison, our model is re-trained each year to include the data from previous years. In the second, our model is trained on 90% of the data from this period, and tested on the remaining 10%. We demonstrate results via confusion matrices (a) and (b) produced using a 0.45 probability cutoff for our hybrid model and (c) the mechanistic model, along with (d) ROC curves and (e) the results of simulating COTS prioritisation. We note here that the mechanistic model's results represent an upper bound on its performance at undersurveyed reefs (see Section 2.5.2). TP = true positive, FN = false negative, FP = false positive, and TP = true positive.

cate temporal trends, namely that the model appears capable of picking up cyclic outbreak wave dynamics at a GBR-wide scale. Importantly, these results do not merely demonstrate that the model can reproduce observations: because survey effort is incomplete and non-random, the purpose of the hindcast is to estimate the latent dynamics underlying the observed, biased sample.

When summarising hindcasts from 1991-2025 at a reef scale (Figure 7), the Swains emerges as the area predicted to sustain the most frequent outbreaks, matching observational data. Following the Swains, the model also identifies a high potential for outbreaks at many reefs in the Initiation Box, central GBR, and northern GBR regions, again in line with observed trends. Furthermore, aside from the far northern region the model consistently predicts a lack of outbreaks on outer-shelf reefs, again matching observed spatial trends.

3.6 Variable importance

The variable importance plot in Figure 8 reveals that the most important predictors are the predicted larval settlement and COTS densities at a reef over the 6 years prior to prediction. Together, these predictors are responsible for approximately 22% of the model's predictive accuracy. These are followed by predicted recent coral cover, predicted COTS history, recent degree heating weeks, recent regional culling effort, recent sea-surface temperature, and recent chlorophyll-a concentration. These 6 predictors collectively account for a further 46% of accuracy approximately, leaving those predictors outside the top 8 contributing 32%.

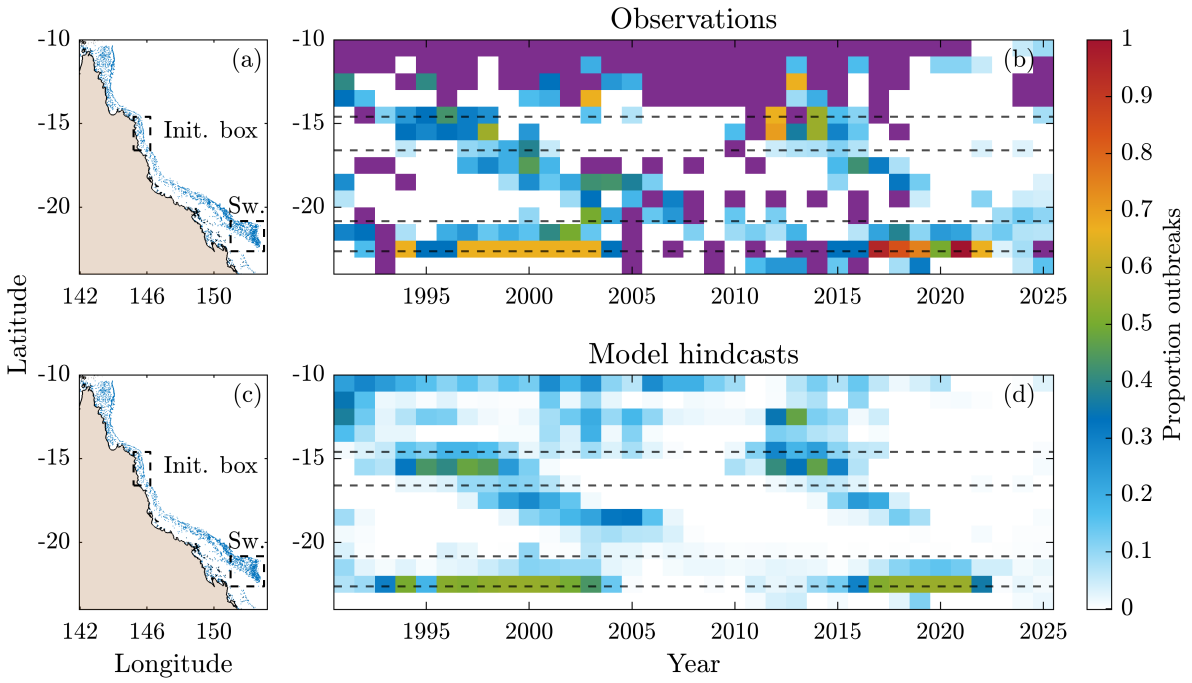

Figure 6: Comparison of GBR-wide hybrid model hindcasts and observations by the proportion of (b) outbreaks predicted (using a 0.45 probability cutoff) or observed (d), aggregated at each latitudinal degree. Regions with insufficient observational data (n < 3) are coloured purple. Maps of the GBR (a, c) are included for reference, highlighting the Initiation box and the Swains regions.

3.7 2026 forecasts

The forecasts displayed in Figure 9 predict that many reefs within the initiation box, Pompeys, and Swains regions have a high potential for sustaining outbreaking densities in 2026. When ranking reefs by their outbreak potential, the majority of the top 200 reefs are found within these regions, with the rest of the GBR predicted to have a significantly lower potential. These regions differ however in how their outbreak potential has changed since 2024, with a mix of increases and decreases in the Pompeys and Swains but a clear concentration of increases in the initiation box.

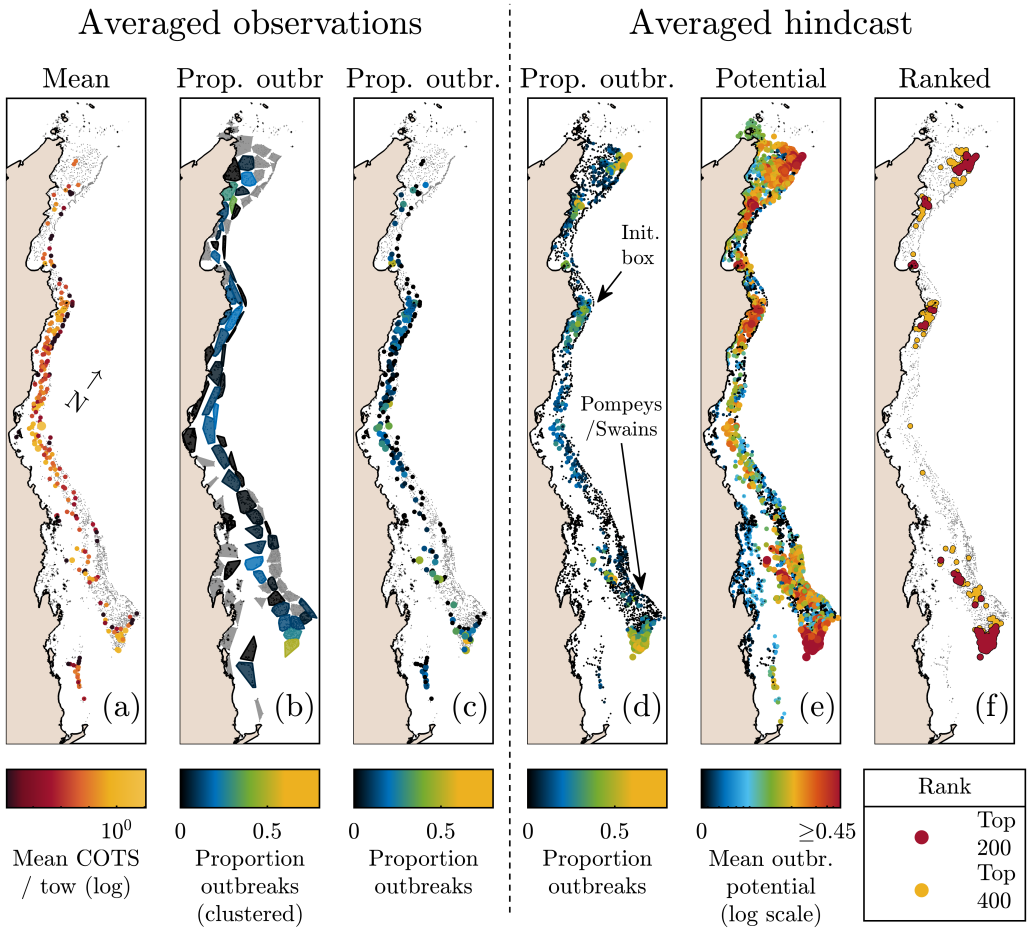

Figure 7: Comparison of COTS observations (a)-(c) with model hindcasts (d)-(f) averaged between 1991 and 2025. Plot (a) shows the mean COTS densities observed, while (b) and (c) show the proportion of those observations for which densities were at outbreak levels at a reef cluster and individual reef scale, respectively. 100 reef clusters were formed using k-means clustering based on spatial position, albeit separately for each shelf position (inner, middle, outer). For plots (a) and (c), only reefs with at least 6 observations are shown, and for plot (b) only clusters with observations at least 7 years are shown (insufficient data in grey). Plot (d) displays the predicted proportion of outbreaks from 1991-2025, where reefs that exceed an outbreak potential of 0.45 for a given year are classed as outbreaks. Plot (e) shows the mean outbreak potential for each reef, which is then ranked in plot (f) highlighting the top 200 ($\approx 5\%$) and 400 ($\approx 10\%$) reefs.

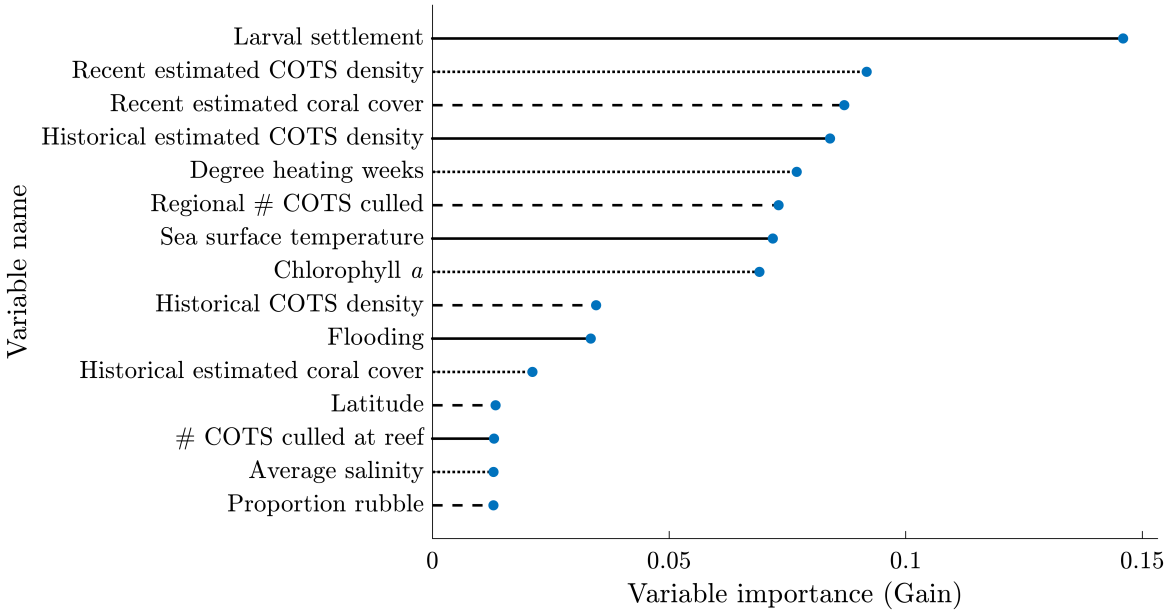

Figure 8: Sorted and aggregated variable importance measures for each predictor or group thereof, with a full list of predictors contained in Appendices A and B. Predictors measuring the same quantity at different years prior to the prediction (e.g. have suffix "Tt", or are summed) are aggregated in the plot above. For ease of interpretability, model variable names have been converted as follows: Larval settlement = conAutocov, Recent estimated COTS density = cotsPerTowImput, Recent estimated coral cover = corCov, Historical estimated COTS density = cotsHistoryImput, Degree heating weeks = dhw, Regional # COTS culled = totCulledRegion, Sea surface temperature = sst, Chlorophyll a = chlA, Historical COTS density = cotsHistory, Flooding = floodExtent, Historical estimated coral cover = coralHistoryImput, Latitude = y, # COTS culled at reef = totCulled, Average salinity = salAve, Proportion rubble = rubbleProp.

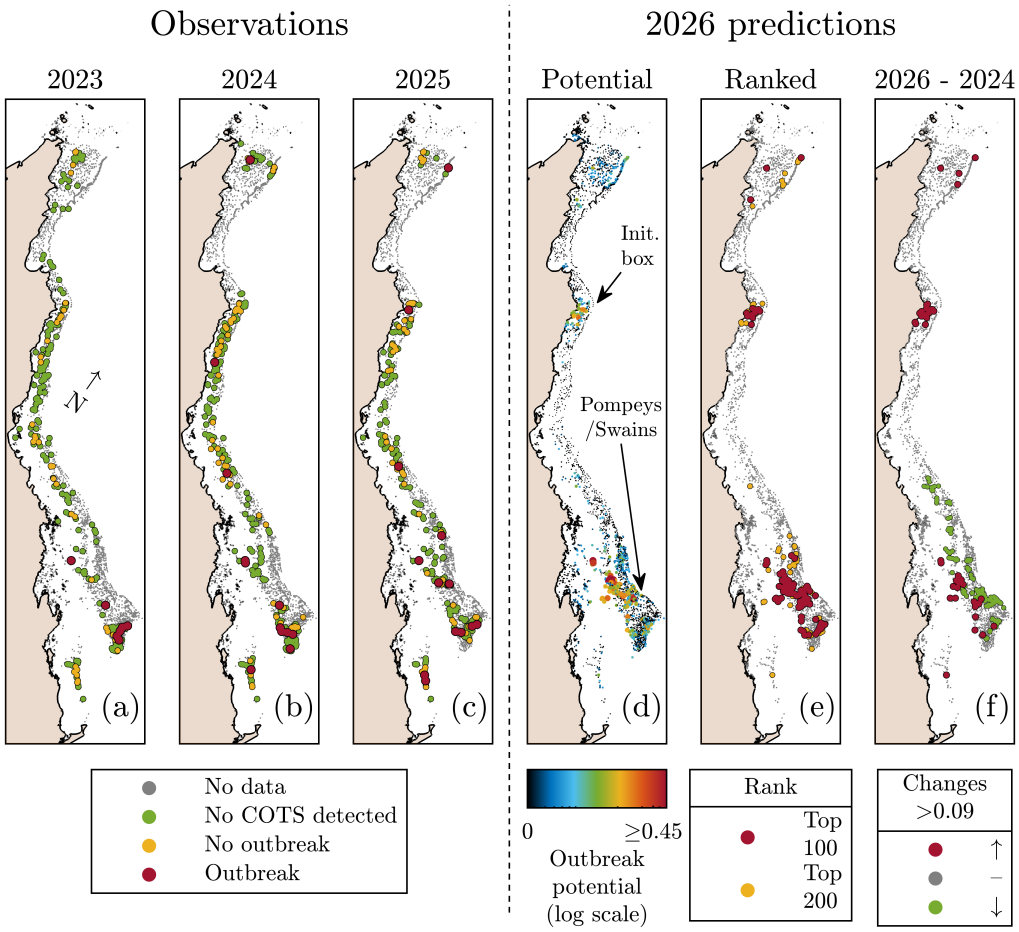

Figure 9: Comparison of COTS observations from 2023 to 2025 (a)-(c) with modelled outbreak predictions for 2026 (d)-(f) formed using data from 1985-2025. Subplot (d) visualises the predicted potential that each reef experiences an outbreak, with values above 0.45 indicating a high-risk of an outbreak occurring. Plot (e) highlights the top 100 and 200 reefs by outbreak potential, and (f) maps changes in outbreak potential by subtracting the 2024 potential from the 2026 potential. Only changes in potential of magnitude > 0.09 are shown representing 20% of the outbreak potential cutoff for binary classification (0.45), with increases in red and decreases in green.

4 Discussion

Predicting when and where population irruptions will occur is critical for effective management, yet their nonlinear dynamics and incomplete surveillance records can limit the performance of conventional mechanistic and statistical models. Here, we show that a hybrid machine-learning approach can improve predictions of COTS outbreaks, in some cases by substantial margins, relative to the mechanistic and statistical approaches considered. In addition to improving predictive skill, the hybrid model provides a comprehensive spatiotemporal reconstruction of past outbreak dynamics across the entire GBR, allowing for a better mapping of historical COTS impacts. Through variable importance analyses, the model also identifies the environmental and ecological predictors most influential in shaping predicted outbreak dynamics.

When predicting forward into 2026 from prior data (1985-2025), the model identifies emerging risks in the initiation box that have been increasing since 2024 (Figure 9). These predictions suggest the beginning of new wave of outbreaks, both broadly aligning with independent reports from the area (Chandler et al. 2023; Uthicke et al. 2024) and also completing them – the model provides comprehensive and spatially explicit predictions for all reefs, including many that have not been surveyed. This provides managers with a basis for directing limited surveillance and control effort towards the most at-risk reefs.

The hybrid model uses a boosted regression architecture, which has a limited capacity to explain its predictions. Nevertheless, our analyses of variable importance provide supporting evidence toward several leading hypotheses regarding COTS population dynamics. To begin with, both chlorophyll and SST proved influential predictors, suggesting that their influence on larval development and survival demonstrated in ex situ experiments (Wolfe et al. 2015; Caballes et al. 2017b; Kamya et al. 2014; Lamare et al. 2014; Pratchett et al. 2017b; Uthicke et al. 2018) may translate to in situ dynamics at the scale of the GBR. Alongside the influence of the flood plume exposure and larval dispersal predictors, these results provide support for the theory that primary outbreaks are affected by a combination of elevated nutrient content and localised dispersal (Wooldridge & Brodie 2015).

From a management perspective, the importance of dispersal and regional culling variables mirror the empirical analyses of Matthews et al. (2024) that indicate culling suppresses larval production and thus impedes outbreak propagation (Hock et al. 2014; Stewart et al. 2026). Our results also support the local, reef-level benefits of culling, however its variable importance was lower than that of regional culling. This should not necessarily be interpreted as evidence that local control is ineffective on the culled reefs themselves. Rather, it likely reflects both the distribution of culling effort in the data and the way BRT variable importance is calculated: because most reefs in the dataset do not receive local culling, variation in local culling effort explains relatively little of the model's aggregate predictive performance. In contrast, regional culling varies across a broader set of reefs/years and may therefore contribute more strongly to overall model accuracy.

More broadly, our results demonstrate the importance of quantifying and including connectivity when modelling metapopulations, made possible here by the hybrid modelling framework. Not only were the connectivity autocovariates the most influential predictors in our model (Figure 8), but multiple other top predictors (SST, chlorophyll, regional culling) utilised spatial averages tuned using COTS dispersal models (110 km radius, Stewart et al. 2026). Connectivity also plays a central role in models of other irruptive species (Powell & Bentz 2014; Shatz et al. 2016; Zhang et al. 2023), supporting the findings of studies that quantify the benefits of including dispersal in ecological population models (Sullivan et al. 2012; Holloway et al. 2016; Parreira et al. 2023). Our results also reflect the findings of Wesselkamp et al. (2024), who demonstrate that hybrid modelling in ecology can offer improvements in predictive accuracy over alternative approaches.

While the hybrid model improves prediction accuracy relative to the alternative approaches, its outputs remain probabilistic estimates of outbreak potential rather than direct observations of outbreak state. Accordingly, when predictions are converted into a binary outbreak/no-outbreak classification, the model can miss a substantial proportion of outbreaking reefs and produce false-alarms at others. Another limitation is the model's reliance on recent observations across the GBR to accurately forecast outbreaks, which could reduce the model's accuracy were spatiotemporal data gaps to emerge. This is likely due to the model's most influential predictor (conAutocovTt) relying on local COTS population data, which when absent reduces the model's predictive ability. A good example is the notable reduction in model accuracy in the far northern GBR, a region with significantly lower surveillance effort than elsewhere. However, going forward an increase

in spatiotemporal gaps is unlikely given the gradual increase in COTS control resources.

The model was designed to support tactical COTS-management at the spatial and temporal scales at which decisions are made: identifying reefs with elevated outbreak potential over the coming year to inform surveillance and control effort as outbreaks propagate. This near-term focus allows predictions to be based on environmental, connectivity, and management conditions similar to those represented in the training data. Its application to longer forecasting horizons is therefore less certain, highlighting a constraint of hybrid models applied to systems with nonstationary conditions. Namely, that ML-based approaches cannot extrapolate well to conditions not represented in their training data. This is especially pertinent for the GBR, where climate change is altering environmental conditions and disturbance regimes to place the system in previously unfamiliar states. Similar issues can arise when simulating counterfactuals, if doing so pushes predictors into uncharted territory. In these cases mechanistic models may be more appropriate tools for both longer-term predictions and scenario analysis, provided they exhibit sufficient accuracy.

Predictor uncertainty is a further limitation. Our larval-settlement predictor (conAutocovTt) omits density-dependent fertilisation and settlement, which may influence COTS reproduction but remain insufficiently quantified for empirical parameterisation (Babcock & Mundy 1992; Rogers et al. 2017; Pratchett et al. 2017a). Likewise, our cyclone metric does not capture the spatially variable effects of storm winds, waves, and reef geomorphology represented in more sophisticated exposure models (e.g., Holland et al. 2010). The model also necessarily omits or simplifies relevant processes, including predation pressure on COTS (Sweatman 2008; Doll et al. 2026), temporally variable turbidity, and the depth-dependent temperature and chlorophyll conditions experienced by larvae; the latter are represented here using surface remote-sensing estimates despite larvae occurring across a broad depth range (Huang et al. 2024; Sun et al. 2024; Uthicke et al. 2026).

This study shows that hybrid modelling can provide a practical middle ground between purely mechanistic and purely correlative approaches for forecasting population irruptions. For COTS on the GBR, embedding mechanistic information on larval connectivity within a flexible machine-learning model improved short-term outbreak prediction and reconstructed historical outbreak-wave dynamics more effectively than the alternative models considered. The hybrid approach is not intended to replace mechanistic models, which remain valuable for examining system behaviour and management scenarios under explicit assumptions. Nor does it diminish the value of traditional statistical models as transparent and efficient predictive tools. Rather, it demonstrates the benefit of combining mechanistic understanding with the capacity of machine learning to learn nonlinear, context-dependent relationships from large, noisy, observational datasets. In systems where management decisions must be made before ecological dynamics are fully understood, hybrid models offer a way to turn partial process knowledge and imperfect observations into timely, testable, and continually improvable decision support.

Statements and declarations

Acknowledgements

The authors would also like to thank Dr Severine Choukroun, Dr Dan Pagendam, Professor Morgan Pratchett, Dr Jennifer Wilmes, Isobel Ryan, Dr David Williamson, and Kailash Cook for various discussions that improved this work.

The authors extend their gratitude to the Great Barrier Reef Marine Park Authority (GBRMPA) for access to COTS control data, and the Australian Institute of Marine Science (AIMS) and GBRMPA for access to COTS monitoring data. The data from AIMS is drawn from the Long Term Monitoring Program (LTMP). The LTMP data analysed in this study were collected from the traditional sea Country of the Gudang Yadhaykenu, Wuthathi, Kuuku Ya'u, Umpila, Dingaal, Thaanill-warra, Ngurruumungu, Eastern Kuku Yalanji, Yirrganydji, Gunggandji, Gunggandji-Mandingalbay yidinji, Mandubarra, Bandjin, Girramay, Gulngay, Djiru, Nywaigi, Manbarra, Wulgurukaba, Bindal, Ngaro, Yuwibara, Wiri, Yuwi-Bara, Koinjmal, Guninmal and Darumbal peoples, as well as people represented by the Mackay Coastal Group and the First Nations Bailai, Gurang, Gooreng Gooreng, Taribelang Bunda Peoples Aboriginal Corporation RNTBC. The authors pay our respects to their Elders past, present and emerging. We also thank all past members and volunteers of the LTMP and the crews of the RV Sirius, RV Harry Messel, RV Lady Basten, RV Cape Ferguson and RV Solander for their excellent logistical support in the field.

Funding

Funding support was provided by the COTS Control Innovation Program through Project RT-06 and Project BR-12. This project contributes to the COTS Control Innovation Program's Bridging Phase, funded by the Australian Government's Reef Trust, the Australian Institute of Marine Science, and the Great Barrier Reef Foundation. DJW is supported by an Australia (ARC) Discovery Early Career Researcher Award (DE250100396).

Supplementary materials

A pre-print version of the Supplementary materials is available at https://github.com/OwenS1919/cotsOutbreakModellingPaper.git under Documents/COTS Outbreak Model Paper - Supps.pdf.

Conflict of interest

The authors have no conflicts of interest to declare.

Availability of data and materials

The COTS monitoring data used in this paper is not publicly available, but can be requested from the Great Barrier Reef Marine Park Authority and the Australian Institute of Marine Science. The remaining code and data is available at https://github.com/OwenS1919/cotsOutbreakModellingPaper.git. The majority of modelling and analysis for this paper was conducted in R (version 4.2.3, R Core Team 2023), with some data processing and all plotting completed in Matlab (version R2023b, The MathWorks Inc. 2023).

References

AIMS (2019). Monitoring the Great Barrier Reef. https://www.aims.gov.au/research-topics/monitoring-and-discovery/monitoring-great-barrier-reef. Accessed: 2019-03-02.

AIMS (2025). Long-term monitoring program. https://www.aims.gov.au/research-topics/monitoring-and-discovery/monitoring-great-barrier-reef/long-term-monitoring-program. Accessed: 2025-01-23.

Ainsworth, T. D., Heron, S. F., Ortiz, J. C., Mumby, P. J., Grech, A., Ogawa, D., Eakin, C. M., and Leggat, W. (2016). Climate change disables coral bleaching protection on the Great Barrier Reef. *Science*, 352(6283):338–342.

Al-Wardy, M., Zarei, E., Nikoo, M. R., and Nazari, R. (2025). Climate-driven projections of cyanobacterial harmful algal bloom expansion in coastal waters. *Science of the Total Environment*, 992:179940.

Allen, J. D., Schrage, K. R., Foo, S. A., Watson, S.-A., and Byrne, M. (2017). The effects of salinity and pH on fertilization, early development, and hatching in the crown-of-thorns seastar. *Diversity*, 9(1):13.

Andersen, R. and Linnell, J. D. (2000). Irruptive potential in roe deer: density-dependent effects on body mass and fertility. *The Journal of wildlife management*, pages 698–706.

Babcock, R. and Mundy, C. (1992). Reproductive biology, spawning and field fertilization rates of acanthatser planci. *Marine and Freshwater Research*, 43(3):525–533.

Babcock, R. C., Plagányi, É. E., Condie, S. A., Westcott, D. A., Fletcher, C. S., Bonin, M. C., and Cameron, D. (2020). Suppressing the next crown-of-thorns outbreak on the Great Barrier Reef. *Coral Reefs*, 39(5):1233–1244.

Baek, S.-S., Kwon, Y. S., Pyo, J., Choi, J., Kim, Y. O., and Cho, K. H. (2021). Identification of influencing factors of a. catenella bloom using machine learning and numerical simulation. *Harmful Algae*, 103:102007.

Bank, W. (2026). The world bank group and the desert locust crisis. https://www.worldbank.org/en/topic/the-world-bank-group-and-the-desert-locust-outbreak. Accessed: 2026-03-09.

Benzie, J. and Dixon, P. (1994). The effects of sperm concentration, sperm: egg ratio, and gamete age on fertilization success in crown-of-thorns starfish (Acanthaster planci) in the laboratory. *The Biological Bulletin*, 186(2):139–152.

Berkelmans, R., De'ath, G., Kininmonth, S., and Skirving, W. J. (2004). A comparison of the 1998 and 2002 coral bleaching events on the Great Barrier Reef: spatial correlation, patterns, and predictions. *Coral reefs*, 23:74–83.

Birkeland, C. (1982). Terrestrial runoff as a cause of outbreaks of Acanthaster planci (Echinodermata: Asteroidea). *Marine biology*, 69:175–185.

Birkeland, C. and Lucas, J. (1990). *Acanthaster planci: major management problem of coral reefs*. CRC press.

BoM (2025). Tropical cyclone databases. http://www.bom.gov.au/cyclone/tropical-cyclone-knowledge-centre/databases/. Accessed: 2025-05-14.

Borthwick, D., Belcher, B., and Hutson, J. (2006). *Review of the Great Barrier Reef Marine Park Act 1975: Review Panel report*. Australian Government.

Bouchard, M. and Auger, I. (2014). Influence of environmental factors and spatio-temporal covariates during the initial development of a spruce budworm outbreak. *Landscape Ecology*, 29(1):111–126.

Bozec, Y.-M., Hock, K., Mason, R. A., Baird, M. E., Castro-Sanguino, C., Condie, S. A., Puotinen, M., Thompson, A., and Mumby, P. J. (2022). Cumulative impacts across Australia's Great Barrier Reef: a mechanistic evaluation. *Ecological monographs*, 92(1):e01494.

Brodie, J., Devlin, M., and Lewis, S. (2017). Potential enhanced survivorship of crown of thorns starfish larvae due to near-annual nutrient enrichment during secondary outbreaks on the central mid-shelf of the Great Barrier Reef, Australia. *Diversity*, 9(1):17.

Brodie, J., Fabricius, K., De'ath, G., and Okaji, K. (2005). Are increased nutrient inputs responsible for more outbreaks of crown-of-thorns starfish? An appraisal of the evidence. *Marine pollution bulletin*, 51(1-4):266–278.

Caballes, C. F., Byrne, M., Messmer, V., and Pratchett, M. S. (2021). Temporal variability in gametogenesis and spawning patterns of crown-of-thorns starfish within the outbreak initiation zone in the northern Great Barrier Reef. *Marine Biology*, 168(1):13.

Caballes, C. F., Pratchett, M. S., and Buck, A. C. (2017a). Interactive effects of endogenous and exogenous nutrition on larval development for crown-of-thorns starfish. *diversity*, 9(1):15.

Caballes, C. F., Pratchett, M. S., Raymundo, M. L., and Rivera-Posada, J. A. (2017b). Environmental tipping points for sperm motility, fertilization, and embryonic development in the crown-of-thorns starfish. *Diversity*, 9(1):10.

Chandler, J. F., Burn, D., Caballes, C. F., Doll, P. C., Kwong, S. L., Lang, B. J., Pacey, K. I., and Pratchett, M. S. (2023). Increasing densities of pacific crown-of-thorns starfish (acanthaster cf. solaris) at Lizard Island, northern Great Barrier Reef, resolved using a novel survey method. *Scientific Reports*, 13(1):19306.

Cheal, A. J., MacNeil, M. A., Emslie, M. J., and Sweatman, H. (2017). The threat to coral reefs from more intense cyclones under climate change. *Global change biology*, 23(4):1511–1524.

Chen, C.-M., Drovandi, C. C., Keith, J. M., Anthony, K., Caley, M. J., and Mengersen, K. (2017). Bayesian semi-individual based model with approximate Bayesian computation for parameters calibration: Modelling Crown-of-Thorns populations on the Great Barrier Reef. *Ecological Modelling*, 364:113–123.

Chen, T., He, T., Benesty, M., Khotilovich, V., Tang, Y., Cho, H., Chen, K., Mitchell, R., Cano, I., Zhou, T., et al. (2015). Xgboost: extreme gradient boosting. *R package version 0.4-2*, 1(4):1–4.

Choukroun, S., Stewart, O. B., Mason, L. B., and Bode, M. (2025). Larval dispersal predictions are highly sensitive to hydrodynamic modelling choices. *Coral Reefs*, 44(1):1–13.

Condie, S. A., Plagányi, É. E., Morello, E. B., Hock, K., and Beeden, R. (2018). Great Barrier Reef recovery through multiple interventions. *Conservation Biology*, 32(6):1356–1367.

Cook, K., Skinner, C., Bozec, Y.-M., and Mumby, P. J. (2026). Marine heatwaves disrupt the culling of crown-of-thorns starfish on the Great Barrier Reef. *Coral Reefs*, pages 1–16.

Cuomo, S., Di Cola, V. S., Giampaolo, F., Rozza, G., Raissi, M., and Piccialli, F. (2022). Scientific machine learning through physics–informed neural networks: Where we are and what's next. *Journal of scientific computing*, 92(3):88.

Deveson, T. and Hunter, D. (2002). The operation of a gis-based decision support system for australian locust management. *Insect Science*, 9(4):1–12.

Devlin, M., McKinna, L., Álvarez-Romero, J., Petus, C., Abott, B., Harkness, P., and Brodie, J. (2012). Mapping the pollutants in surface riverine flood plume waters in the Great Barrier Reef, Australia. *Marine pollution bulletin*, 65(4-9):224–235.

De'ath, G., Fabricius, K. E., Sweatman, H., and Puotinen, M. (2012). The 27–year decline of coral cover on the Great Barrier Reef and its causes. *Proceedings of the National Academy of Sciences*, 109(44):17995–17999.

Doll, P. C., Tebbett, S. B., Ling, S. D., Coenradi, S. L., Burn, D., Hoey, A. S., Emslie, M. J., and Pratchett, M. S. (2026). Elevated predation on crown-of-thorns starfish in no-take marine reserves. *Current Biology*, 36(3):R83–R84.

Doll, P. C., Uthicke, S., Caballes, C. F., Diaz-Pulido, G., Abdul Wahab, M. A., Lang, B. J., Jeong, S. Y., and Pratchett, M. S. (2023). Settlement cue selectivity by larvae of the destructive crown-of-thorns starfish. *Biology Letters*, 19(1):20220399.

Edwards, H. J., Elliott, I. A., Eakin, C. M., Irikawa, A., Madin, J. S., McField, M., Morgan, J. A., Van Woesik, R., and Mumby, P. J. (2011). How much time can herbivore protection buy for coral reefs under realistic regimes of hurricanes and coral bleaching? *Global Change Biology*, 17(6):2033–2048.

Fabricius, K. and De'ath, G. (2001). Environmental factors associated with the spatial distribution of crustose coralline algae on the Great Barrier Reef. *Coral reefs*, 19:303–309.

Fabricius, K., Okaji, K., and De'Ath, G. (2010). Three lines of evidence to link outbreaks of the crown-of-thorns seastar Acanthaster planci to the release of larval food limitation. *Coral reefs*, 29:593–605.

FAO (2022). Progress report on the response in the Greater Horn of Africa and Yemen, September–December 2021. Technical report, Food and Agricultural Organisation of the United Nations.

Fletcher, C., Bonin, M., and Westcott, D. (2020). An ecologically-based operational strategy for cots control: integrated decision making from the site to the regional scale. *Report to the National Environmental Science Programme. Reef and Rainforest Research Centre Limited, Cairns.*

Fletcher, C. S., Castro-Sanguino, C., Condie, S., Bozec, Y., Hock, K., Gladish, D., Mumby, P., and Westcott, D. (2021). Regional-scale modelling capability for assessing crown-of-thorns starfish control strategies on the Great Barrier Reef. *Report to the National Environmental Science Program. Reef and Rainforest Research Centre Limited.*

Frölicher, T. L., Fischer, E. M., and Gruber, N. (2018). Marine heatwaves under global warming. *Nature*, 560(7718):360–364.

GBRMPA (2024a). Crown-of-thorns starfish control program annual work plan 2024-2025. Technical report.

GBRMPA (2024b). Crown-of-thorns starfish project dashboard. https://www2.gbrmpa.gov.au/our-work/programs-and-projects/crown-thorns-starfish-management/crown-thorns-starfish-project-dashboard. Accessed: 2024-09-04.

Geoscience Australia (2017). Ausbathytopo (Great Barrier Reef) 30m 2017 - a regional-scale depth model (20170025c). https://ecat.ga.gov.au/geonetwork/srv/eng/catalog.search#/metadata/115066. Accessed: 2025-04-23.

Goroshko, A. A., Sultson, S. M., Ponomarev, E. I., Demidko, D. A., Slinkina, O. A., Mikhaylov, P. V., Tatarintsev, A. I., Kulakova, N. N., and Khizhniak, N. P. (2025). Risk modeling for the emergence of the primary outbreak area of the siberian moth dendrolimus sibiricus tschetv. in coniferous forests of central siberia. *Forests*, 16(1):160.

Hardy, N. A., Lamare, M., Uthicke, S., Wolfe, K., Doo, S., Dworjanyn, S., and Byrne, M. (2014). Thermal tolerance of early development in tropical and temperate sea urchins: inferences for the tropicalization of eastern Australia. *Marine Biology*, 161:395–409.

Hock, K., Wolff, N. H., Condie, S. A., Anthony, K. R. N., and Mumby, P. J. (2014). Connectivity networks reveal the risks of crown-of-thorns starfish outbreaks on the Great Barrier Reef. *Journal of Applied Ecology*, 51(5):1188–1196.

Hock, K., Wolff, N. H., Ortiz, J. C., Condie, S. A., Anthony, K. R. N., Blackwell, P. G., and Mumby, P. J. (2017). Connectivity and systemic resilience of the Great Barrier Reef. *PLOS Biology*, 15(11):e2003355.

Holland, G. J., Belanger, J. I., and Fritz, A. (2010). A revised model for radial profiles of hurricane winds. *Monthly weather review*, 138(12):4393–4401.

Holloway, P., Miller, J. A., and Gillings, S. (2016). Incorporating movement in species distribution models: how do simulations of dispersal affect the accuracy and uncertainty of projections? *International Journal of Geographical Information Science*, 30(10):2050–2074.

Howe, M., Graham, E. E., and Nelson, K. N. (2024). Defoliator outbreaks track with warming across the Pacific coastal temperate rainforest of North America. *Ecography*, 2024(9):e07370.

Huang, Z., Brooke, B., Whitta, N., Potter, A., Fuller, M., Dunn, J., and Pitcher, R. (2010). Australian marine physical environmental data—descriptions and metadata. *Geoscience Australia Record*, 32.

Huang, Z., Feng, M., Dalton, S. J., and Carroll, A. G. (2024). Marine heatwaves in the Great Barrier Reef and Coral Sea: their mechanisms and impacts on shallow and mesophotic coral ecosystems. *Science of the Total Environment*, 908:168063.

Hughes, T. P., Kerry, J. T., Álvarez-Noriega, M., Álvarez-Romero, J. G., Anderson, K. D., Baird, A. H., Babcock, R. C., Beger, M., Bellwood, D. R., Berkelmans, R., et al. (2017). Global warming and recurrent mass bleaching of corals. *Nature*, 543(7645):373–377.

Hughes, T. P., Kerry, J. T., Baird, A. H., Connolly, S. R., Dietzel, A., Eakin, C. M., Heron, S. F., Hoey, A. S., Hoogenboom, M. O., Liu, G., et al. (2018). Global warming transforms coral reef assemblages. *Nature*, 556(7702):492–496.

Islam, M. Z., Fletcher, C. S., Sun, K., Dezfouli, A., and Chades, I. (2026). Leveraging sparse observations to predict species abundance across space and time. In *Proceedings of the AAAI Conference on Artificial Intelligence*, volume 40, pages 38616–38625.

Jiménez, J. E., Feinsinger, P., and Jaksić, F. M. (1992). Spatiotemporal patterns of an irruption and decline of small mammals in northcentral Chile. *Journal of Mammalogy*, 73(2):356–364.

Johnson, C. (1992). Settlement and recruitment of acanthatser planci on the Great Barrier Reef: Questions of process and scale. *Australian journal of marine and freshwater research*, 43(3):611–627.

Johnson, C. R., Sutton, D., Olson, R., and Giddins, R. (1991). Settlement of crown-of-thorns starfish: role of bacteria on surfaces of coralline algae and a hypothesis for deepwater recruitment. *Marine ecology Progress series*, pages 143–162.

Kamya, P. Z., Dworjanyn, S. A., Hardy, N., Mos, B., Uthicke, S., and Byrne, M. (2014). Larvae of the coral eating crown-of-thorns starfish, Acanthaster planci in a warmer-high CO2 ocean. *Global Change Biology*, 20(11):3365–3376.

Kroon, F. J., Barneche, D. R., and Emslie, M. J. (2021). Fish predators control outbreaks of crown-of-thorns starfish. *Nature Communications*, 12(1):6986.

Lamare, M., Pecorino, D., Hardy, N., Liddy, M., Byrne, M., and Uthicke, S. (2014). The thermal tolerance of crown-of-thorns (Acanthaster planci) embryos and bipinnaria larvae: implications for spatial and temporal variation in adult populations. *Coral Reefs*, 33:207–219.

Lawrence, E., Foster, S. D., Matthews, S. A., Williamson, D., Pratchett, M. S., Doyle, J., Bainbridge, S., Uthicke, S., Doll, P. C., Kusy, B., et al. (2026). A quantitative comparison of tools for monitoring the abundance of crown-of-thorns starfish and coral cover. *Coral Reefs*, pages 1–15.

Lawton, D., Scarth, P., Deveson, E., Piou, C., Spessa, A., Waters, C., and Cease, A. J. (2022). Seeing the locust in the swarm: accounting for spatiotemporal hierarchy improves ecological models of insect populations. *Ecography*, 2022(2).

Li, M., MacLean, D. A., Hennigar, C. R., and Ogilvie, J. (2020). Previous year outbreak conditions and spring climate predict spruce budworm population changes in the following year. *Forest Ecology and Management*, 458:117737.

Lubiana Botelho, L., Jeynes-Smith, C., Vollert, S. A., and Bode, M. (2025). Calibrated ecosystem models cannot predict the consequences of conservation management decisions. *Ecology Letters*, 28(1):e70034.

Lucas, J. (1973). Reproductive and larval biology of Acanthaster planci (L.) in Great Barrier Reef waters. *Micronesica*, 9(2):197–203.

Lucas, J. (1982). Quantitative studies of feeding and nutrition during larval development of the coral reef asteroid Acanthaster planci (L.). *Journal of Experimental Marine Biology and Ecology*, 65(2):173–193.

Lucas, J. (1984). Growth, maturation and effects of diet in Acanthaster planci (L.)(Asteroidea) and hybrids reared in the laboratory. *Journal of Experimental Marine Biology and Ecology*, 79(2):129–147.

MacLean, D., Erdle, T., MacKinnon, W., Porter, K., Beaton, K., Cormier, G., Morehouse, S., and Budd, M. (2001). The spruce budworm decision support system: forest protection planning to sustain long-term wood supply. *Canadian Journal of Forest Research*, 31(10):1742–1757.

Mamo, D. K., Kinyanjui, M. N., and Siewe, N. (2025). Mathematical assessment of the role of temperature on desert locust population dynamics. *Plos one*, 20(1):e0317040.

Massel, S. and Done, T. (1993). Effects of cyclone waves on massive coral assemblages on the Great Barrier Reef: meteorology, hydrodynamics and demography. *Coral Reefs*, 12:153–166.

Matthews, S., Mellin, C., and Pratchett, M. S. (2020a). *Larval connectivity and water quality explain spatial distribution of crown-of-thorns starfish outbreaks across the Great Barrier Reef*, page 223–258. Elsevier.

Matthews, S., Shoemaker, K., Pratchett, M. S., and Mellin, C. (2020b). COTSMod: A spatially explicit metacommunity model of outbreaks of crown-of-thorns starfish and coral recovery. In *Advances in Marine Biology*, volume 87, pages 259–290. Elsevier.

Matthews, S. A., Bode, M., Beeden, R., Bonin, M. C., Fletcher, C. S., Kerrigan, B., Ryan, I., Wilmes, J., White, A., and Williamson, D. H. (2026). Operationalising resilience-based management at scale: A meta-adaptive blueprint from the Great Barrier Reef crown-of-thorns starfish control program. *Biological Conservation*, 321:111910.

Matthews, S. A., Mellin, C., MacNeil, A., Heron, S. F., Skirving, W., Puotinen, M., Devlin, M. J., and Pratchett, M. (2019). High-resolution characterization of the abiotic environment and disturbance regimes on the Great Barrier Reef, 1985–2017.

Matthews, S. A., Williamson, D. H., Beeden, R., Emslie, M. J., Abom, R. T., Beard, D., Bonin, M., Bray, P., Campili, A. R., Ceccarelli, D. M., et al. (2024). Protecting Great Barrier Reef resilience through effective management of crown-of-thorns starfish outbreaks. *Plos one*, 19(4):e0298073.

Mellin, C., Matthews, S., Anthony, K. R., Brown, S. C., Caley, M. J., Johns, K. A., Osborne, K., Puotinen, M., Thompson, A., Wolff, N. H., et al. (2019). Spatial resilience of the Great Barrier Reef under cumulative disturbance impacts. *Global change biology*, 25(7):2431–2445.

Miller, I. R., Jonker, M., and Coleman, G. (2019). Crown-of-thorns starfish and coral surveys using the manta tow technique. *Long-term monitoring of the Great Barrier Reef standard operational procedure*, 9:1–41.

Mills, C. E. (2001). Jellyfish blooms: are populations increasing globally in response to changing ocean conditions? *Hydrobiologia*, 451(1):55–68.

Moran, P., De'Ath, G., Baker, V., Bass, D., Christie, C., Miller, I., Miller-Smith, B., and Thompson, A. (1992). Pattern of outbreaks of crown-of-thorns starfish (acanthaster planci l.) along the Great Barrier Reef since 1966. *Marine and Freshwater Research*, 43(3):555–567.

Moran, P. J. (1988). *The acanthaster phenomenon*.

NASA (2025). Ocean colour web. https://oceancolor.gsfc.nasa.gov. Accessed: 2025-04-12.

NOAA (2025a). Daily global 5km satellite coral bleaching heat stress monitoring (version 3.1, 1985-present, released august 1, 2018). https://www.star.nesdis.noaa.gov/pub/socd/mecb/crw/data/5km/v3.1_op/nc/v1.0/annual/. Accessed: 2025-04-12.

NOAA (2025b). NOAA High-resolution Blended Analysis of Daily SST and Ice. https://psl.noaa.gov/data/gridded/data.noaa.oisst.v2.highres.html. Accessed: 2025-04-01.

Novak, M., Wootton, J. T., Doak, D. F., Emmerson, M., Estes, J. A., and Tinker, M. T. (2011). Predicting community responses to perturbations in the face of imperfect knowledge and network complexity. *Ecology*, 92(4):836–846.

Oliver, E. C. J., Donat, M. G., Burrows, M. T., Moore, P. J., Smale, D. A., Alexander, L. V., Benthuysen, J. A., Feng, M., Sen Gupta, A., Hobday, A. J., Holbrook, N. J., Perkins-Kirkpatrick, S. E., Scannell, H. A., Straub, S. C., and Wernberg, T. (2018). Longer and more frequent marine heatwaves over the past century. *Nature Communications*, 9(1).

O'Mahoney, J., Simes, R., Redhill, D., Heaton, K., Atkinson, C., Hayward, E., and Nguyen, M. (2017). At what price? the economic, social and icon value of the Great Barrier Reef.

Ørsted, M., Lye, J., Umina, P. A., and Maino, J. L. (2021). Global analysis of the seasonal abundance of the invasive pest drosophila suzukii reveal temperature extremes determine population activity potential. *Pest Management Science*, 77(10):4555–4563.

Osborne, K., Dolman, A. M., Burgess, S. C., and Johns, K. A. (2011). Disturbance and the dynamics of coral cover on the Great Barrier Reef (1995–2009). *PLOS ONE*, 6(3):1–10.

Parreira, M. R., Tessarolo, G., and Nabout, J. C. (2023). Incorporating symmetrical and asymmetrical dispersal into ecological niche models in freshwater environments. *Acta Limnologica Brasiliensia*, 35:e16.

Piou, C. and Marescot, L. (2023). Spatiotemporal risk forecasting to improve locust management. *Current Opinion in Insect Science*, 56:101024.

Plaisance, L., Caley, M. J., Brainard, R. E., and Knowlton, N. (2011). The diversity of coral reefs: what are we missing? *PloS one*, 6(10):e25026.

Powell, J. A. and Bentz, B. J. (2014). Phenology and density-dependent dispersal predict patterns of mountain pine beetle (dendroctonus ponderosae) impact. *Ecological Modelling*, 273:173–185.

Pratchett, M., Caballes, C., Wilmes, J., Matthews, S., Mellin, C., Sweatman, H., Nadler, L., Brodie, J., Thompson, C., Hoey, J., Bos, A., Byrne, M., Messmer, V., Fortunato, S., Chen, C., Buck, A., Babcock, R., and Uthicke, S. (2017a). Thirty years of research on crown-of-thorns starfish (1986–2016): Scientific advances and emerging opportunities. *Diversity*, 9(4):41.

Pratchett, M. S. (2007). Feeding Preferences of Acanthaster planci (Echinodermata: Asteroidea) under Controlled Conditions of Food Availability. *Pacific Science*, 61(1):113–120.

Pratchett, M. S., Baird, A. H., Burn, D., Caballes, C. F., Chandler, J. F., Garing, M., Lang, B. J., Levering, L. T., Pacey, K. I., and Doll, P. C. (2026). Detectability of Pacific crown-of-thorns starfish (Acanthaster cf. solaris) using scooter-assisted large area diver-based (SALAD) surveys in the Northern Great Barrier Reef, Australia. *Coral Reefs*, pages 1–11.

Pratchett, M. S., Caballes, C. F., Burn, D., Doll, P. C., Chandler, J. F., Doyle, J. R., and Uthicke, S. (2022). Scooter-assisted large area diver-based (SALAD) visual surveys to test for renewed outbreaks of crown-of-thorns starfish (Acanthaster cf. solaris) in the northern Great Barrier Reef. *A report to the Australian Government by the COTS Control Innovation Program*, 32.

Pratchett, M. S., Caballes, C. F., Rivera-Posada, J. A., and Sweatman, H. P. (2014). *Limits to Understanding and Managing Outbreaks of Crown- of- Thorns Starfish (Acanthaster spp.)*, page 133–200. CRC Press.

Pratchett, M. S., Chandler, J. F., Choukroun, S. M., Doll, P. C., Lang, B. J., Kwong, S., Chen, C. C., Emslie, M. J., Caballes, C. F., Uthicke, S., and Matthews, S. A. (2024). *Biophysical Processes Involved in the Initiation and Spread of Population Irruptions of Crown-of-Thorns Starfish on the Great Barrier Reef*. CRC press.

Pratchett, M. S., Dworjanyn, S., Mos, B., Caballes, C. F., Thompson, C. A., and Blowes, S. (2017b). Larval survivorship and settlement of crown-of-thorns starfish (Acanthaster cf. solaris) at varying algal cell densities. *Diversity*, 9(1):2.

R Core Team (2023). R: A language and environment for statistical computing, version 4.2.3 (2023-03-15 ucrt).

Raissi, M., Perdikaris, P., and Karniadakis, G. E. (2019). Physics-informed neural networks: A deep learning framework for solving forward and inverse problems involving nonlinear partial differential equations. *Journal of Computational physics*, 378:686–707.

Ramazi, P., Kunegel-Lion, M., Greiner, R., and Lewis, M. A. (2021). Predicting insect outbreaks using machine learning: A mountain pine beetle case study. *Ecology and evolution*, 11(19):13014–13028.

Reaka-Kudla, M. L. et al. (1997). The global biodiversity of coral reefs: a comparison with rain forests. *Biodiversity II: Understanding and protecting our biological resources*, 2:551.

Roberts, T., Moloney, J., Sweatman, H., and Bridge, T. (2015). Benthic community composition on submerged reefs in the central Great Barrier Reef. *Coral Reefs*, 34:569–580.

Roelfsema, C. M., Lyons, M. B., Castro-Sanguino, C., Kovacs, E. M., Callaghan, D., Wettle, M., Markey, K., Borrego-Acevedo, R., Tudman, P., Roe, M., et al. (2021). How much shallow coral habitat is there on the Great Barrier Reef? *Remote Sensing*, 13(21):4343.

Rogers, J. G., Pláganyi, É. E., and Babcock, R. C. (2017). Aggregation, allee effects and critical thresholds for the management of the crown-of-thorns starfish acanthaster planci. *Marine Ecology Progress Series*, 578:99–114.

Royama, T. (1984). Population dynamics of the spruce budworm choristoneura fumiferana. *Ecological Monographs*, 54(4):429–462.

Shatz, A. J., Rogan, J., Sangermano, F., Miller, J., and Elmes, A. (2016). Modeling the risk of spread and establishment for asian longhorned beetle (anoplophora glabripennis) in massachusetts from 2008-2009. *Geocarto International*, 31(8):813–831.

Sheppard, C. (1982). Coral populations on reef slopes and their major controls. *Mar Ecol Prog Ser*, 7:83–115.

Silva, A., Pinto, L., Rodrigues, S., De Pablo, H., Santos, M., Moita, T., and Mateus, M. (2016). A hab warning system for shellfish harvesting in portugal. *Harmful Algae*, 53:33–39.

Skinner, C., Bozec, Y.-M., Matthews, S. A., Williamson, D. H., Beeden, R., and Mumby, P. J. (2024). Advancing projections of crown-of-thorns starfish to support management interventions. *Science of The Total Environment*, 950:175282.

Small, A., Adey, W. H., and Spoon, D. (1998). Are current estimates of coral reef biodiversity too low? the view through the window of a microcosm. *Atoll Research Bulletin*.

Srivastava, V., Tai, A. R., Robert, J. A., and Carroll, A. L. (2024). A dynamic outbreak distribution model (dodm) for an irruptive folivore: the western spruce budworm. *Ecological Modelling*, 492:110737.

Stewart, O., Downie, A. T., Choukroun, S., and Bode, M. (2026). Larval dispersal models predict reefs that experience crown-of-thorns starfish outbreaks receive more larvae. *Coral Reefs*, pages 1–19.

Stoeckl, N., Hicks, C. C., Mills, M., Fabricius, K., Esparon, M., Kroon, F., Kaur, K., and Costanza, R. (2011). The economic value of ecosystem services in the Great Barrier Reef: our state of knowledge. *Annals of the New York Academy of Sciences*, 1219(1):113–133.

Sturtevant, B. R., Cooke, B. J., Kneeshaw, D. D., and MacLean, D. A. (2015). Modeling insect disturbance across forested landscapes: insights from the spruce budworm. In *Simulation modeling of forest landscape disturbances*, pages 93–134. Springer.

Sullivan, M. J., Davies, R. G., Reino, L., and Franco, A. M. (2012). Using dispersal information to model the species–environment relationship of spreading non-native species. *Methods in ecology and evolution*, 3(5):870–879.

Sun, C., Steinberg, C., Klein Salas, E., Mellin, C., Babcock, R. C., Schiller, A., Cantin, N. E., Stella, J. S., Baird, M. E., Condie, S. A., et al. (2024). Climate refugia in the Great Barrier Reef may endure into the future. *Science Advances*, 10(48):eado6884.

Sweatman, H. (2008). No-take reserves protect coral reefs from predatory starfish. *Current Biology*, 18(14):R598–R599.

Sweatman, H., Delean, S., and Syms, C. (2011). Assessing loss of coral cover on Australia 's Great Barrier Reef over two decades, with implications for longer-term trends. *Coral Reefs*, 30(2):521–531.

The MathWorks Inc. (2023). Matlab version: 23.2.0.2428915 (r2023b) update 4.

UNESCO (2024). Great Barrier Reef. https://whc.unesco.org/en/list/154/. Accessed: 2024-10-30.

Uthicke, S., Doyle, J., Patel, F., Cabrera, M. G., and Schaffelke, B. (2026). Biophysical and eDNA sampling reveals upwelling-enhanced food availability for larvae of the corallivorous crown-of-thorns seastar, Acanthaster cf. solaris. *Marine Pollution Bulletin*, 229:119657.

Uthicke, S., Doyle, J. R., Gomez Cabrera, M., Patel, F., McLatchie, M. J., Doll, P. C., Chandler, J. F., and Pratchett, M. S. (2024). edna monitoring detects new outbreak wave of corallivorous seastar (Acanthaster cf. solaris) at Lizard Island, Great Barrier Reef. *Coral Reefs*, 43(4):857–866.

Uthicke, S., Liddy, M., Patel, F., Logan, M., Johansson, C., and Lamare, M. (2018). Effects of larvae density and food concentration on crown-of-thorns seastar (Acanthaster cf. solaris) development in an automated flow-through system. *Scientific reports*, 8(1):642.

Vanhatalo, J., Hosack, G. R., and Sweatman, H. (2016). Spatiotemporal modelling of crown-of-thorns starfish outbreaks on the Great Barrier Reef to inform control strategies. *Journal of Applied Ecology*, 54(1):188–197.

Veran, S., Simpson, S. J., Sword, G. A., Deveson, E., Piry, S., Hines, J. E., and Berthier, K. (2015). Modeling spatiotemporal dynamics of outbreaking species: influence of environment and migration in a locust. *Ecology*, 96(3):737–748.

Vercelloni, J., Caley, M. J., and Mengersen, K. (2017). Crown-of-thorns starfish undermine the resilience of coral populations on the Great Barrier Reef. *Global Ecology and Biogeography*, 26(7):846–853.

Von Rueden, L., Mayer, S., Sifa, R., Bauckhage, C., and Garcke, J. (2020). Combining machine learning and simulation to a hybrid modelling approach: Current and future directions. In *International symposium on intelligent data analysis*, pages 548–560. Springer.

Wesselkamp, M., Moser, N., Kalweit, M., Boedecker, J., and Dormann, C. F. (2024). Process-informed neural networks: A hybrid modelling approach to improve predictive performance and inference of neural networks in ecology and beyond. *Ecology letters*, 27(11):e70012.

Wilmes, J. C., Schultz, D. J., Hoey, A. S., Messmer, V., and Pratchett, M. S. (2020). Habitat associations of settlement-stage crown-of-thorns starfish on Australia's Great Barrier Reef. *Coral Reefs*, 39(4):1163–1174.

Wolanski, E., Richmond, R., McCook, L., and Sweatman, H. (2003). Mud, marine snow and coral reefs: the survival of coral reefs requires integrated watershed-based management activities and marine conservation. *American Scientist*, 91(1):44–51.

Wolfe, K., Graba-Landry, A., Dworjanyn, S. A., and Byrne, M. (2015). Larval starvation to satiation: Influence of nutrient regime on the success of Acanthaster planci. *PloS one*, 10(3):e0122010.

Wolfe, K., Graba-Landry, A., Dworjanyn, S. A., and Byrne, M. (2017). Superstars: Assessing nutrient thresholds for enhanced larval success of Acanthaster planci, a review of the evidence. *Marine Pollution Bulletin*, 116(1-2):307–314.

Wood, S. N. and Thomas, M. B. (1999). Super–sensitivity to structure in biological models. *Proceedings of the Royal Society of London. Series B: Biological Sciences*, 266(1419):565–570.

Wooldridge, S. A. and Brodie, J. E. (2015). Environmental triggers for primary outbreaks of crown-of-thorns starfish on the Great Barrier Reef, Australia. *Marine pollution bulletin*, 101(2):805–815.

Xiao, X., He, J., Huang, H., Miller, T. R., Christakos, G., Reichwaldt, E. S., Ghadouani, A., Lin, S., Xu, X., and Shi, J. (2017). A novel single-parameter approach for forecasting algal blooms. *Water research*, 108:222–231.

Yan, Z., Kamanmalek, S., Alamdari, N., and Nikoo, M. R. (2024). Comprehensive insights into harmful algal blooms: a review of chemical, physical, biological, and climatological influencers with predictive modeling approaches. *Journal of Environmental Engineering*, 150(4):03124002.

Young, I. and Hardy, T. (1993). Measurement and modelling of tropical cyclone waves in the Great Barrier Reef. *Coral Reefs*, 12:85–95.

Youngblood, J. P., Cease, A. J., Talal, S., Copa, F., Medina, H. E., Rojas, J. E., Trumper, E. V., Angilletta Jr, M. J., and Harrison, J. F. (2023). Climate change expected to improve digestive rate and trigger range expansion in outbreaking locusts. *Ecological Monographs*, 93(1):e1550.

Zahir, M., Su, Y., Shahzad, M. I., Ayub, G., Rahman, S. U., and Ijaz, J. (2024). A review on monitoring, forecasting, and early warning of harmful algal bloom. *Aquaculture*, 593:741351.

Zhang, B., Leroux, S. J., Bowden, J. J., Hargan, K. E., Hurford, A., and Moise, E. R. (2023). Species distribution model identifies influence of climatic constraints on severe defoliation at the leading edge of a native insect outbreak. *Forest Ecology and Management*, 544:121166.

Zhang, L., Lecoq, M., Latchininsky, A., and Hunter, D. (2019). Locust and grasshopper management. *Annual review of entomology*, 64(1):15–34.

Appendix A Covariates List

Table 2: List of predictors used in our model and their associated sources and citations. Note that some rows refer to multiple predictors in the model, as some include individual values for multiple preceding years. This is indicated by the suffix Tt, where predictorT5 would indicate the value of the predictor 5 years before the year being predicted. For these variables, t spans from 1 to 6 aside from chlATt and sstTt which span from 2 to 6. All variables that include a sum across t are taken across all t values unless otherwise specified. These summations ignore any missing values, with summations inflated accordingly if missing values are present to retain comparability. The spatial autocovariate is also calculated for multiple different distances, indicated by the suffix R$r$km for r at 25 and 125. Additional predictors from Matthews et al. (2020a) were also included, and are detailed in Section B.

Code	Description	Units	Years	Source	COTS Reference
coralHabProp	Proportion of reef predicted to be coral habitat, with missing values imputed using a spatial KNN and GBR-average	0-1	2018	Roelfsema et al. (2021)	
spatAutocovR$r$kmTt	Spatial autocovariate, estimates the average COTS density to the north, south, and region surrounding a focal reef at multiple distances r and prior years t, along with the sum over t Note: not used in outbreak model, used instead in COTS density imputation	COTS per manta tow	1986-2025	Calculated using COTS manta tow data	Pratchett et al. (2024) Vanhatalo et al. (2016)
conAutocovTt	Connectivity autocovariate, estimates the amount of COTS larvae arriving at each reef for each prior year t, along with their sum from $t = 3$ to 6	N/A	1986-2025	Calculated using COTS manta tow data and COTS dispersal models Choukroun et al. (2025)	Stewart et al. (2026)
weightedInStrength	Sum of incoming connectivity probabilities weighted by area of source reef	N/A	N/A	Calculated using COTS dispersal models Choukroun et al. (2025)	

Code	Description	Units	Years	Source	COTS Reference
inDegree	Number of nonzero incoming connectivity probabilities	N/A	N/A	Calculated using COTS dispersal models Choukroun et al. (2025)	
cotsPerTowMed	Median observed COTS density for reefs with 2 or more observations	COTS per manta tow	1986-2025	Calculated using COTS manta tow data	
cotsPerTowMean	Mean observed COTS density for reefs with 2 or more observations	COTS per manta tow	1986-2025	Calculated using COTS manta tow data	
cotsPerTowMax	Maximum observed COTS density for reefs with 2 or more observations	COTS per manta tow	1986-2025	Calculated using COTS manta tow data	
cotsPerTowMedImput	Imputed median observed COTS density using a spatial KNN based on the cotsPerTowMed variable	COTS per manta tow	1986-2025	Calculated using COTS manta tow data	
cotsPerTowMeanImput	Imputed mean observed COTS density using a spatial KNN based on the cotsPerTowMean variable	COTS per manta tow	1986-2025	Calculated using COTS manta tow data	
cotsPerTowMaxImput	Imputed maximum observed COTS density using a spatial KNN based on the cotsPerTowMax variable	COTS per manta tow	1986-2025	Calculated using COTS manta tow data	
corCovTt	Imputed percentage hard coral cover at a reef for preceding years $t$using a spatial KNN based on observational data	%	1986-2025	Calculated using COTS manta tow data	
corCovMin	Minimum observed hard coral cover for reefs with 2 or more observations	%	1986-2025	Calculated using COTS manta tow data	
corCovMean	Mean observed hard coral cover for reefs with 2 or more observations	%	1986-2025	Calculated using COTS manta tow data	
corCovMax	Maximum observed hard coral cover for reefs with 2 or more observations	%	1986-2025	Calculated using COTS manta tow data	

Code	Description	Units	Years	Source	COTS Reference
corCovMinImput	Imputed median observed hard coral cover using a spatial KNN based on the corCovMin variable	%	1986-2025	Calculated using COTS manta tow data	
corCovMeanImput	Imputed mean observed hard coral cover using a spatial KNN based on the corCovMean variable	%	1986-2025	Calculated using COTS manta tow data	
corCovMaxImput	Imputed maximum observed hard coral cover using a spatial KNN based on the corCovMax variable	%	1986-2025	Calculated using COTS manta tow data	
totCulledTt	Total number of COTS culled from a reef divided by the area of the reef for prior years t, along with their sum	COTS/ m^2	1986-2025	Calculated using COTS culling data	Matthews et al. (2024)
totCulledRegionTt	Total number of COTS culled within a 110 km radius of a reef for prior years t along with their sum	COTS	1986-2025	Calculated using COTS culling data	Matthews et al. (2024)
chlATt	Average surface Chlorophyll a concentration in a 110 km radius of each reef between December-February inclusive, for prior years t along with their sum from $t = 3$ to 6	$\mu g\, L^{-1}$	2002-2025	NASA (2025)	Fabricius et al. (2010) Uthicke et al. (2018) Wolfe et al. (2015, 2017) Pratchett et al. (2017b)
sstTt	Average sea-surface temperature in a 110 km radius of each reef between December-February inclusive, for prior years t along with their sum from $t = 3$ to 6	°C	1981-2024	NOAA (2025b)	Caballes et al. (2017b) Lamare et al. (2014) Kamya et al. (2014)
dhwTt	Average yearly degree-heating weeks experienced by a reef for prior years t, along with their sum from $t = 3$ to 6	DHW	1986-2024	NOAA (2025a)	Hughes et al. (2017) Cook et al. (2026)
area	Area of a reef	m^2	N/A		
perim	Perimeter of a reef, calculated using points at least 50 m apart to counter the coastline paradox	m	N/A		

Code	Description	Units	Years	Source	COTS Reference
aveDepth	Average depth of a reef	m	N/A	Geoscience Australia (2017)	Wilmes et al. (2020) Doll et al. (2023)
dist2Shore	Minimum distance from reef to shore	km	N/A		Vanhatalo et al. (2016) Fabricius & De'ath (2001)
shelfPos	Shelf position – Inner, outer, mid	categorical	N/A	Matthews et al. (2020a)	Vanhatalo et al. (2016)
x	Longitude of reef centroid	°			Vanhatalo et al. (2016)
y	Latitude of reef centroid	°			Vanhatalo et al. (2016)
cycImpact$t$	Yearly cumulative wind speed experienced by reefs due to cyclonic activity for prior years t, along with their sum	mh/s	1980-2024	BoM (2025)	
rubbleProp	Proportion of reef predicted to be rubble, with missing values imputed using a spatial KNN and GBR-average	0-1	2018	Roelfsema et al. (2021)	Wilmes et al. (2020)
cotsPerTowImputTt	Imputed COTS per tow density at a reef over multiple prior years t using a spatial KNN based on observational data, including the sum from $t = 3$ to 6	COTS/tow	1986-2025	Calculated using COTS manta tow data	

Appendix B Matthews et al. (2020a) predictors list

Table 3: List of predictors used by Matthews et al. (2020a) and their associated sources that we use in our models. Variable categories are environmental (Env), water quality (WQ), spatial (Spat), coral (Cor), disturbance (Dist), connectivity (Conn), and auto-covariates (Auto Cov).

Type	Code	Description	Units	Years	Source	COTS Reference
Env	o2Ave	Average oxygen	mLL^{-1}	1960-2006	Huang et al. (2010) Matthews et al. (2019)	Lamare et al. (2014) Hardy et al. (2014)
Env	no3Ave	Average nitrate	µM	1960-2006		Birkeland & Lucas (1990)
Env	salAve	Average salinity	PSU	1960-2006		Lucas (1973) Allen et al. (2017) Caballes et al. (2017b)
Env	salSR	Seasonal range salinity	PSU	1960-2006		
Env	waveStress	Percentage of time for which the bed shear stress was >0.4 Pa Wave exposure proxy	%	2010		Moran (1988)
Env	mud	percentage of a seabed sediment sample that is <63 µm in diameter	%	1960-2009		Wolanski et al. (2003)
WQ	floodPrim	Primary (representing turbid, sediment dominated plume) flood plume frequency (weeks occurred / total weeks) during wet season max = 26). – relative frequency	0–1	2000-2014	Devlin et al. (2012) Matthews et al. (2019)	Fabricius et al. (2010) Wolfe et al. (2015) Wooldridge & Brodie (2015) Pratchett et al. (2017b) Brodie et al. (2017)
WQ	floodSec	Secondary chlorophyll dominated plume–relative frequency	0–1	2000-2014		

Type	Code	Description	Units	Years	Source	COTS Reference
WQ	floodTer	Further extent of plume, as delineated by salinity <34 ppt—relative frequency	0–1	2000-2014		
Spat	shelfPos	Cross shelf location (Inner, Middle, Outer)	Factor (3 Levels)	N/A	AIMS (2019)	Moran (1988)
Spat	zone	Open or closed to fishing	Factor (2 Levels)	N/A	GBRMPA	Sweatman (2008) Vanhatalo et al. (2016) Kroon et al. (2021)
Cor	corComm	Benthic coral community type	Factor (6 Levels)	Estimated 2018	Mellin et al. (2019)	Lucas (1984) Pratchett (2007) Caballes et al. (2017a)
Cor	corHardMax	Predicted maximum coral cover	0–100%	Estimated 2018		Lucas (1984) Caballes et al. (2017a)
Dist	bleachExp	Mean exposure to 1998 and 2002 bleaching events	1–5	1998, 2002	Berkelmans et al. (2004) Matthews et al. (2019)	Hughes et al. (2018)